Supporting Information

Two Novel MOF-74 Analogs Exhibiting Unique Luminescent Selectivity

Gui-lei Liu, Yong-jie Qin, Lei Jing, Gui-yuan Wei, and Hui Li*

Key Laboratory of Cluster Science of Ministry of Education, School of Chemistry, Beijing Institute of Technology, Beijing 100081, P. R. China.

*E-mail address: lihui@bit.edu.cn

Tel: 86-10-68912667

Contents

Section 1	Materials and Instrumentation	p. S3
Section 2	Synthesis of Compounds **1** and **2**	p. S3
Section 3	Single-crystal X-ray Crystallography	p. S4
Section 4	Experiment of Photoluminescence (PL) Investigations	p. S4
Section 5	Crystal Data and Selected Bond Distances and Angles of **1** and **2**	p. S6
Section 6	Structural Information for **1** and **2**	p. S7
Section 7	IR spectrum, TGA Curves and PXRD Patterns for **1** and **2**	p. S11
Section 8	UV-vis and PL spectra of free ligands, **1**, **1a**, **2**, and **2a**	p. S14
Section 9	PL spectra of ligands, ligands+metals and normalized PL spectra of ligands, ligands+metals and MOF-desolvated	p. S23
Section 10	TGA Curves of 1⊃Solvents and 2⊃Solvents	p. S32
Section 11	Gas sorption isotherms of MOF **1a** and **2a** for N_2	p.S41

Section 1. Materials and Instrumentation.

All reagents and solvents were used as received from commercial suppliers without further purification. (E)-3-(2-hydroxyl-phenyl)-acrylic acid, (E)-3-(3-hydroxyl-phenyl)-acrylic acid and 4,4'-pyridine were purchased from the company of Alfa Aesar China (Tianjin). Organic solvents with analytical purity were supplied by commercial sources and used as received. Elemental analyses (C, H, N) were performed on a Flash EA1112 microanalyzer at the Beijing Institute of Technology. FT-IR spectrum is recorded in the Nicolet-360 FT-IR spectrometer as KBr pellets in the 4000–400 cm^{-1} region. The UV-vis absorption spectra were examined on a JASCO UV-1901 spectrophotometer in the wavelength range of 200~800 nm. The photoluminescence (PL) spectra were recorded by using a Hitachi F-7000 luminescence spectrophotometer equipped with a 450 W xenon lamp as the excitation source, and the measurements were performed at room temperature. The photomultiplier tube voltage was 700 V, the scan speed was 12000 $nm \cdot min^{-1}$, and the slit width was 2.5 nm. Thermo-gravimetric analysis (TGA) were carried out on a SEIKO TG/DTA 6200 thermal analyzer from room temperature to 1000 °C at a ramp rate of 10 °C/min in a flowing 150 mL/min nitrogen atmosphere. X-ray powder diffraction (XPRD) of samples were measured using a Japan Rigaku D/max γ A X-ray diffractometer equipped with graphite-monochromatized Cu Kα radiation (λ = 0.154060 nm). Nitrogen adsorption experiments and micropore analysis were conducted at 77K using a TriStarII3020 (Micromeritics Instrument Corporation) apparatus. Before adsorption measurements, the samples were degassed in vacuum at 333K for 2h and 403K for 6h. The specific surface areas (SSAs) of the freeze-dried samples were calculated by Brunauer Emmett Teller (BET) analyses of their adsorption isotherms.

Section 2. Synthesis of compounds 1, 2, 1⊃Solvents and 2⊃Solvents.

Synthesis of $\{[Zn(OCA{-}OH)_2(4,4'\text{-bipy})_{0.5}]\cdot 1.67H_2O$ (1)$\}_n$. A mixture of OCA-OH (0.025g, 0.15mmol) and triethlamine (15.1mg, 0.15 mmol) was dissolved in methanol solution (6 mL) to bring the pH of the solution to about 7 with constantly stirring for thirty minutes and then a methanol solution (6 mL) of $Zn(ClO_4)_2 \cdot 6H_2O$ (0.027g, 0.075mmol) was added whilst stirring. To this solution 4-4'-bipyridine (7.8 mg, 0.05 mmol) in Dimethyl sulfoxide solution (1mL) was added with stirring for 30 minutes. The result solution was then filtered and left at ambient condition for three days and the colorless prism single crystals suitable for X-ray diffraction were obtained with the yield of 63% based on $Zn(ClO_4)_2 \cdot 6H_2O$. Anal. Calcd for $C_{23}H_{21.33}NZnO_{7.67}$: C, 55.23; H, 4.30; N, 2.80. Found: C, 55.86; H, 4.13; N, 2.99.

Synthesis of $\{[Zn(MCA{-}OH)_2(4,4'\text{-bipy})_{0.5}]\cdot 0.5CH_3OH\cdot H_2O$ (2)$\}_n$. A solution of $Zn(ClO_4)_2 \cdot 6H_2O$ (0.054g, 0.15mmol) in CH_3OH (6ml) was added to the solution of (E)-3-(3-hydroxyl-phenyl)-acrylic acid (MCA-OH) (0.049g, 0.30mmol)in CH_3OH (6ml) adjusted with triethylamine(0.30mmol) to pH ≈ 7 with constantly stirring for thirty minutes. Then, a solution of 4,4'-bipyridine(0.015g, 0.10mmol) was added to the mixture with constantly stirring for fifteen minutes. The result solution was then filtered and left at room temperature. The single crystals (colorless prisms)

suitable for X-ray diffraction were obtained by slow evaporation for three days and washed with CH_3OH several times to give $[Zn(MCA{-}OH)_2(4,4'\text{-bipy})_{0.5}]\cdot 0.5CH_3OH\cdot H_2O$, yield 75%. Anal. Calcd for $C_{23.5}H_{22}NZnO_{7.5}$: C, 55.98; H, 4.40; N, 2.78. Found: C, 57.05; H, 3.83; N, 2.94.

Synthesis of 1⊃Solvents and 2⊃Solvents. In a Pyrex reaction tube, dried complex **1** (30mg) was prepared by evacuation at 60 ºC for 2 h, and then 130 ºC for 5 h; subsequently, it was immersed in CH_3CN (1 ml) at room temperature. After excess CH_3CN was completely removed by evacuation at room temperature for 5 h, the reaction tube was filled with nitrogen. **1**⊃CH_3OH, **1**⊃CH_3CH_2OH, **1**⊃acetone, **1**⊃CH_2Cl_2, **1**⊃H_2O, **1**⊃THF, **1**⊃cyclohexane, **2**⊃CH_3CN, **2**⊃CH_3OH, **2**⊃CH_3CH_2OH, **2**⊃acetone, **2**⊃CH_2Cl_2, **2**⊃H_2O, **2**⊃THF, **2**⊃cyclohexane, **2**⊃C_6H_6, **2**⊃$C_6H_6CH_3$, **2**⊃C_6H_6I and **2**⊃$C_6H_6NO_2$ were prepared same way by using corresponding guest solvent molecules, respectively.

Section 3. Single-crystal X-ray crystallography.

Suitable single crystals with dimensions of 0.25 × 0.07 × 0.07 mm and 0.50 × 0.14 × 0.14 mm for compounds **1** and **2** were selected for single-crystal X-ray diffraction analysis respectively. Data collection were performed on a Rigaku RAXIS-RAPID CZN diffractometer equipped with a graphite-monochromatic Mo Kα radiation (λ =0.71073 Å) using an ω scan mode for compounds **1** and **2** at 153(2) K. Unit-cell parameters were determined from automatic centering of 25 reflections and refined by a least-squares method. All non-hydrogen atoms were located by direct methods and subsequent difference Fourier syntheses. The hydrogen atoms bound to carbon were located by geometrical calculations, and their positions and thermal parameters were fixed during structure refinement. All non-hydrogen atoms were refined by full-matrix least-squares techniques with $I > 2\sigma(I)$. All refinements were performed using SHELXTL 97. The isolated solvent atom O9 and O7 are disordered to three positions (O9/O9'/O9'' and O7/O7'/O7'') in compounds **1** and **2** respectively. In compound **1**, the restraint command ''ISOR'' was applied to the disordered O9 atom for obtaining reasonable thermal parameters. In compound **2**, the restraint command ''ISOR'' was applied to the disordered C2, C6, C6', C7, C7', O7'', O8, C24 and C24' atoms, and the restraint command "EADP" is applied to the disordered O4, O4', C7, C7', C24 and C24' atoms for obtaining reasonable thermal parameters. The bond distance restraint command "DFIX" is applied to the bonds C24−O8, C24'−O8, C7−C8 and C7'−O8 for obtaining reasonable bond distances. In compound **2**, the two MCA-OH ligands are each equally disordered over two orientations, the refined occupancies have values 0.502(7) and 0.498(7) which do not differ from an exact 0.5 value. It is acceptable to only refine half-occupancy O and C atoms isotropically. CCDC-890826 (**1**) and CCDC-890827 (**2**) contain the supplementary crystallographic data for this paper. These data can be obtained free of charge from The Cambridge Crystallographic Data Centre via www.ccdc.cam.ac.uk/data_request/cif.

Section 4. Experiment of Photoluminescence (PL) investigations.

The fluorescence properties of compounds **1**, **2**, **1a** and **2a** in the solid state, and those of

desolvated **1** and **2** in various solvent emulsions (designated as **1a**-solvent and **2a**-solvent respectively) were investigated at room temperature. Desolvated **1** and **2** were prepared as follows: after immersed in CH_3OH for 3 days, the sample was evacuated at 60 ℃ for 1 h and then 120. ℃ for over 3h. The **1a**-solvent and **2a**-solvent emulsions were prepared by introducing 1.0 mg of **1a**-solvent and **2a**-solvent fine powder into 50 mL of MeOH, EtOH, CH_3CN, CH_2Cl_2, DMF, DMSO, THF, distilled water, acetone, or cyclohexane respectively. After sonication treatment, aging for over 24 h and shaking, the fluorescence spectra were measured. For sensing properties with respect to solvents, desired amounts of desolvated-**1** emulsion in distilled water (0.4 mg of fine powder of desolvated-**1** in 10 mL of in distilled water) were added into a certain requirement amount of desolvated-**1** emulsion in acetone (0.4 mg of fine powder of desolvated-**1** in 10 mL of acetone), and desired amounts of desolvated-**2** emulsion in distilled water (0.4 mg of fine powder of desolvated-**2** in 10 mL of in distilled water) were added into a standard desolvated-**2** emulsion in acetonitrile (0.4 mg of fine powder of desolvated-**2** in 10 mL of acetonitrile). The photoluminescence spectra were investigated after sonication treatment, one-day aging and shaking vigorously before testing.

For further detecting the sensing properties with respect to solvents, desired amounts of desolvated-**1** emulsion in DMSO (0.4 mg of fine powder of desolvated-**1** in 10 mL of in DMSO) were added into a certain requirement amount of desolvated-**1** emulsion in acetone (0.4 mg of fine powder of desolvated-**1** in 10 mL of acetone), and desired amounts of desolvated-**1** emulsion in distilled water (0.4 mg of fine powder of desolvated-**1** in 10 mL of in distilled water) were added into a standard desolvated-**1** emulsion in methanol (0.4 mg of fine powder of desolvated-**2** in 10 mL of methanol). The photoluminescence spectra were investigated after sonication treatment, one-day aging and shaking vigorously before testing.

To detect luminescence diminishment properties of acetone to **1a**, a small amount of acetone were added into a certain requirement amount of desolvated-**1** emulsion in DMSO and H_2O (0.4 mg of fine powder of desolvated-**1** in 10 mL of in DMSO and H_2O respectively). The photoluminescence spectra were investigated after shaking vigorously.

To detect the solid-state PL properties of guest-free framework **2a** upon immerging to the two different categories of aromatic compounds, namely, compounds containing electron-withdrawing groups such as nitroaromatics (group A) and those having electron-donating groups such as CH_3 (group B), the fine powder of **2**⊃C_6H_6, **2**⊃$C_6H_6CH_3$, **2**⊃C_6H_6I and **2**⊃$C_6H_6NO_2$ with the same amount and similar particle size (the good agreement of the XRPD patterns in intensity and position demonstrates that these powder have similar particle size) were investigated at room temperature.

Luminescence control experiments were done in different small solvent molecules by using the ligands (OCA-OH+4,4'-bipy and MCA-OH+4,4'-bipy), ligands+metals (OCA-OH+4,4'-bipy+ $Zn(ClO_4)_2 \cdot 6H_2O$ and MCA-OH+4,4'-bipy+$Zn(ClO_4)_2 \cdot 6H_2O$) to compare with the emission properties of MOF- desolvated (Zn-OCA-MOF- desolvated (**1a**) and Zn-MCA-MOF- desolvated

(**2a**)) at the same concentration, to see the solvent effect on these different systems.

Section 5. Crystal Data and Selected Bond Distances and Angles of 1 and 2.

Table S1 Crystal Data and Structure Refinement of Compounds **1** and **2.**

Compounds	**1**	**2**
Formula	$C_{23}H_{21.33}NO_{7.67}Zn$	$C_{23.5}H_{22}NO_{7.5}Zn$
*F*w	499.78	503.79
T(K)	153(2)	93(2)
Wavelength (Å)	0.71073	0.71073
Crystal system	*Rhombohedral*	*Rhombohedral*
Space group	*R*-3	*R*-3
a (Å)	31.864(5)	31.8565(9)
b (Å)	31.864(5)	31.8565(9)
c (Å)	12.846(3)	12.6269(6)
α (º)	90.00	90.00
β (º)	90.00	90.00
γ (º)	120.00	120.00
Volume ($Å^{-3}$)	11295(3)	11097.5(7)
Z	18	18
ρ(calculated)/g·cm^{-3}	1.322	1.346
μ(Mo-Kα)/mm^{-1}	1.021	1.039
F (000)	4632	4608
θ Range /°	3.10 – 25.01	3.11 – 25.02
Reflns collected	24909	25327
Independent reflns	4356	4319
Obsd data [I>2σ(I)]	3904	4123
Data / restraints / parameters	4356 / 6 / 320	4319 / 59 / 387
GOF on F^2	1.060	1.083
R1, wR2 [I > 2σ(I)]	0.0625, 0.1523	0.0789, 0.1844
R1, wR2 (all data)	0.0708, 0.1585	0.0829, 0.1870
Δρmax, min/e$Å^{-3}$	1.007, -0.490	0.626, -0.425

Table S2 Selected Bond Distances (Å) and Angles (deg) for **1**

Zn(1)-O(1)	1.949(3)	Zn(1)-O(2)	1.980(3)
Zn(1)-O(3)	1.953(3)	Zn(1)-N(1)	2.052(3)
C(19)-N(1)-Zn(1)	121.2(3)	C(23)-N(1)-Zn(1)	121.3(3)
C(1)-O(1)-Zn(1)	116.9(3)	C(1)#3-O(2)-Zn(1)	136.7(3)
C(10)-O(3)-Zn(1)	108.9(3)	O(1)-Zn(1)-O(3)	128.29(12)
O(1)-Zn(1)-O(2)	96.05(12)	O(3)-Zn(1)-O(2)	118.41(12)
O(1)-Zn(1)-N(1)	113.65(13)	O(3)-Zn(1)-N(1)	97.94(13)
O(2)-Zn(1)-N(1)	99.88(13)		

#3 Symmetry code: -x+y-1/3,-x+1/3,z+1/3

Table S3 Selected Bond Distances (Å) and Angles (deg) for **2**

Zn(1)-O(5)	1.941(5)	Zn(1)-O(3)#1	1.951(4)
Zn(1)-O(2)	1.981(4)	Zn(1)-N(1)	2.050(4)
Zn(1)-O(6')	2.122(4)	O(3)-Zn(1)#2	1.951(4)
O(5)-Zn(1)-O(3)#1	126.0(2)	O(5)-Zn(1)-O(2)	122.4(3)
O(3)#1-Zn(1)-O(2)	92.92(16)	O(5)-Zn(1)-N(1)	99.5(3)
O(3)#1-Zn(1)-N(1)	114.70(17)	O(2)-Zn(1)-N(1)	99.29(17))
O(5)-Zn(1)-O(6')	35.0(2)	O(3)#1-Zn(1)-O(6')	99.37(17))
O(2)-Zn(1)-O(6')	108.51(17)	N(1)-Zn(1)-O(6')	134.5(2)
C(9)-O(2)-Zn(1)	134.5(4)	C(9)-O(3)-Zn(1)#2	115.8(4)
C(18)-O(5)-Zn(1)	110.5(3)	C(18')-O(6')-Zn(1)	101.34(11)
C(23)-N(1)-Zn(1)	122.0(4)	C(19)-N(1)-Zn(1)	120.5(4)

#1 Symmetry code: -y+2/3,x-y-2/3,z+1/3 #2 Symmetry code: -x+y+4/3,-x+2/3,z-1/3

Section 6. Structural Information for 1 and 2.

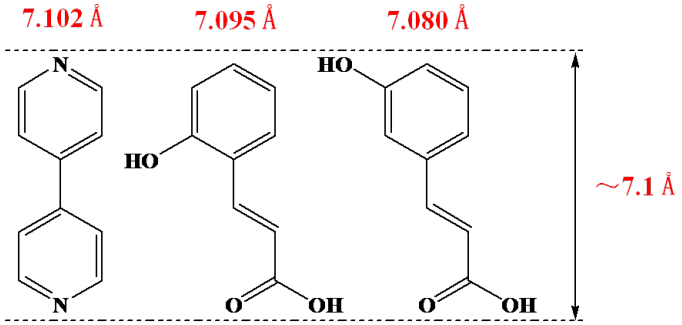

Scheme S1. Lengths of 4,4'-bipy and mono-dentate OCA−OH and MCA−OH ligands in compounds **1** and **2**.

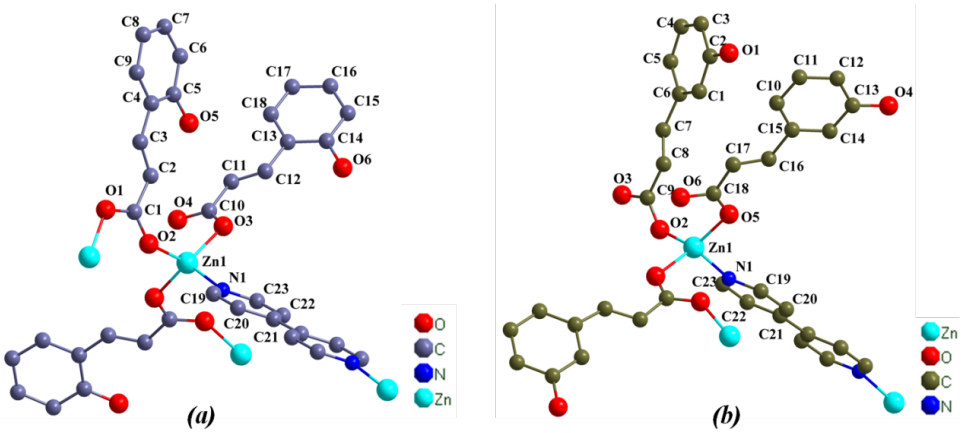

Figure S1. View of the oordination environments of Zn and ligands in (a) **1** and (b) **2**.

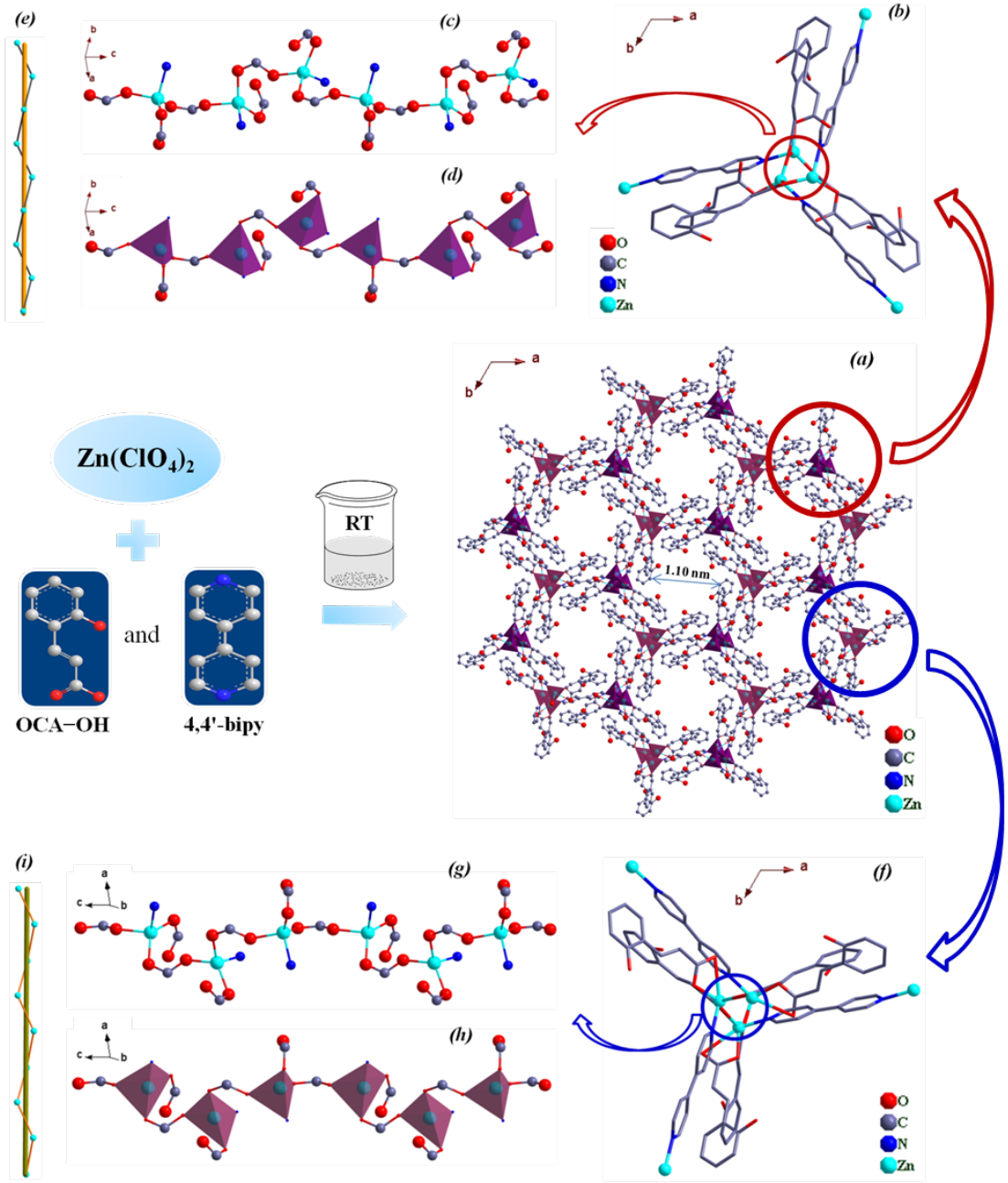

Figure S2. View of (a) the 3D network in **1** along *c*-axis. The different helical chains are highlighted with violet and plum, respectively. (b) View of the 1D left-hand helical chain formed by Zn(II), 4,4'-bipy and OCA-OH ligands in **1**, and (c) the 1D extended chain of Zn(II) ions, and (d) the polyhedral presentation of 1D extended chain of Zn(II) ions, and (e) the left-hand helical presentation in **1**. (f) View of the 1D right-hand helical chain formed by Zn(II), 4,4'-bipy and OCA-OH ligands in **1**, and (g) the 1D extended chain of Zn(II) ions, and (h) the polyhedral presentation of 1D extended chain of Zn(II) ions, and (i) the right-hand helical presentation in **1**. H atoms have been omitted for clarity.

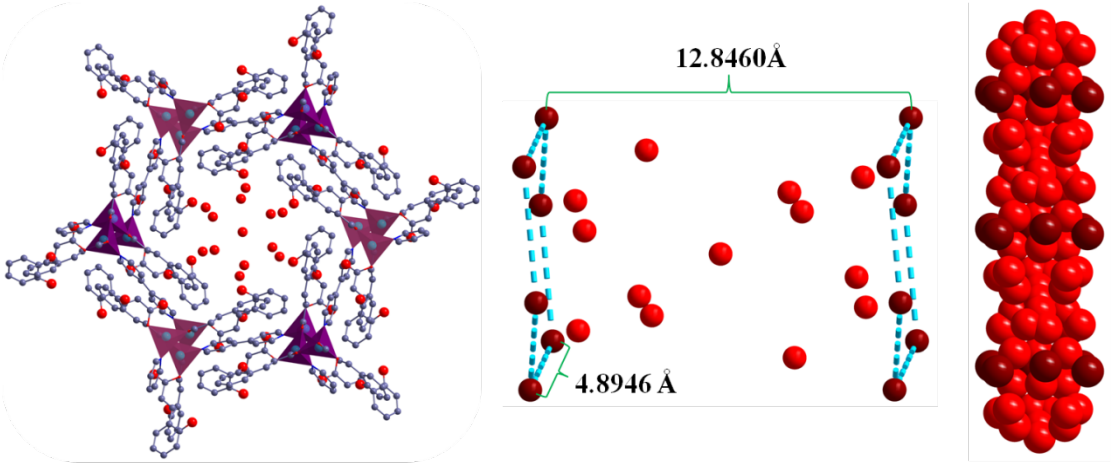

Figure S3. View of the 1D channel presented in (a) **1** which was filled with H_2O solvent molecules. (b) View of the sandwich structure formed by OH groups which showing a chair-shaped configuration and free H_2O molecules in the 1D channel of **1**. (c) View of the space-filling picture of H_2O solvent molecules (red) and OH groups (dark red) along *b*+40° in the 1D channel of **1**. For clarity, the only position was kept for the disordered O atom of H_2O solvent molecules.

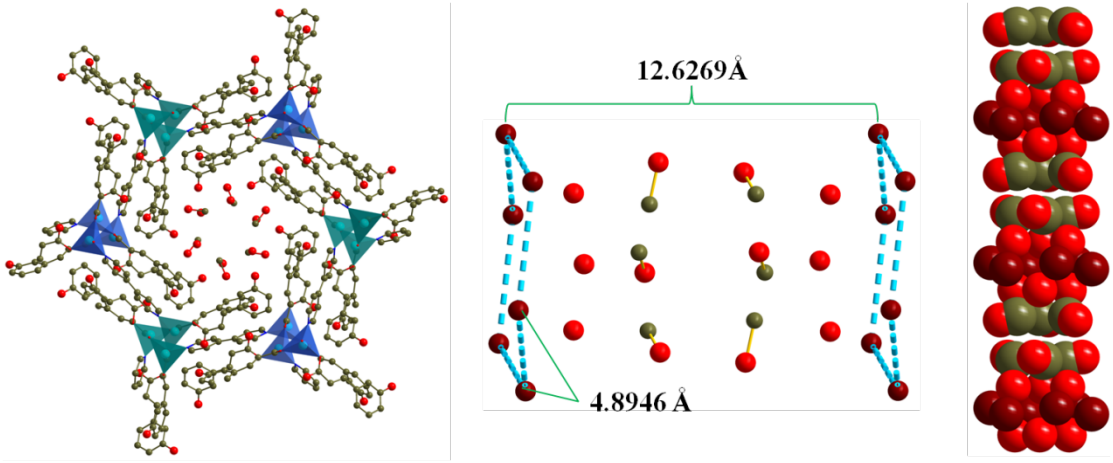

Figure S4. View of the 1D channel presented in (a) **2** which was filled with H_2O and CH_3OH solvent molecules. (b) View of the sandwich structure formed by OH groups which showing a chair-shaped configuration and free H_2O and CH_3OH molecules in the 1D channel of **2**. (c) View of the space-filling picture of H_2O and CH_3OH solvent molecules (O, red; C, olive greeen) and OH groups (dark red) along *b*+30° in the 1D channel of **2**. For clarity, the only position was kept for the disordered MCA-OH ligand and O atoms of H_2O solvent molecules.

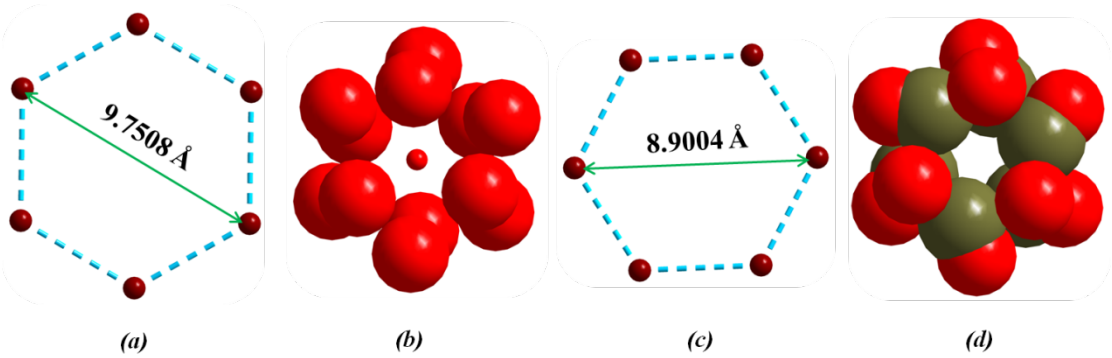

Figure S5. A view showing the different size of 9.7508 Å (a) and 8.9004 Å (b) surrounded by OH groups, and the different dextral (b) and levorotary (d) propeller shape of the H_2O and H_2O, CH_3OH solvent molecules in the 1D channel of **1** and **2** respectively.

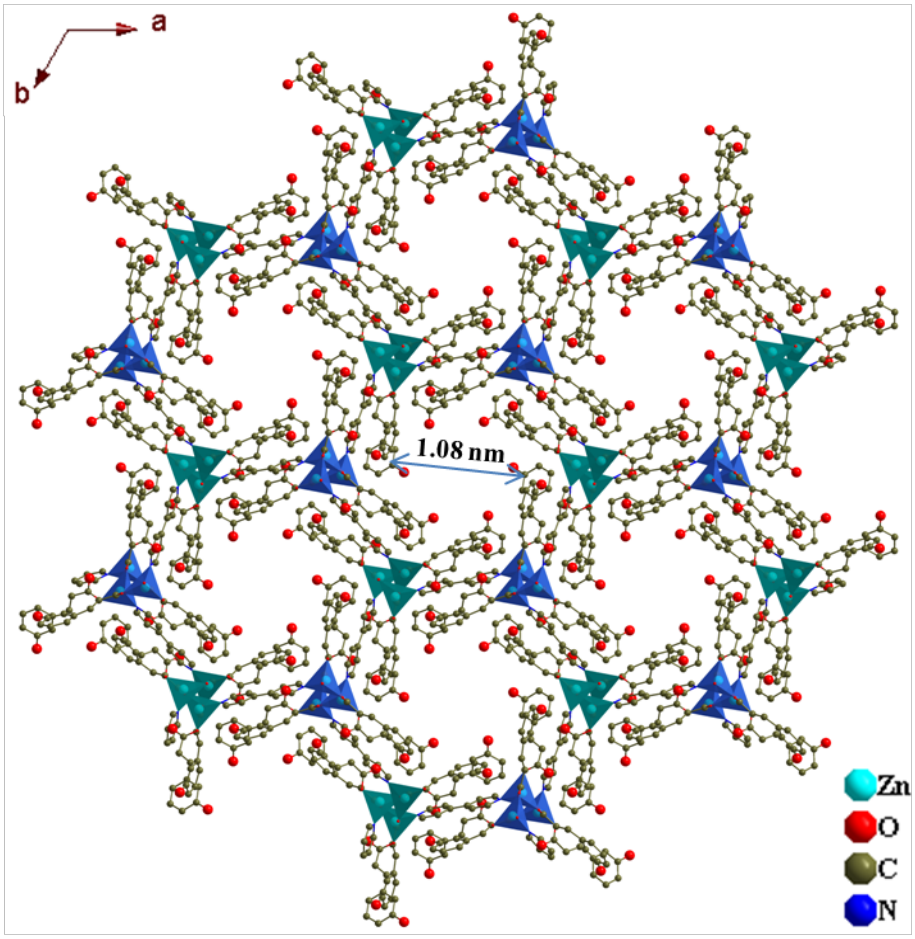

Figure S6. View of the 3D network of **2** along *c*-axis. The different helical chains are highlighted with teal (right-hand) and light blue (left-hand), respectively. For clarity, the only position was kept for the disordered MCA-OH ligands.

Section 7. IR spectrum, TGA Curves and PXRD patterns for 1 and 2.

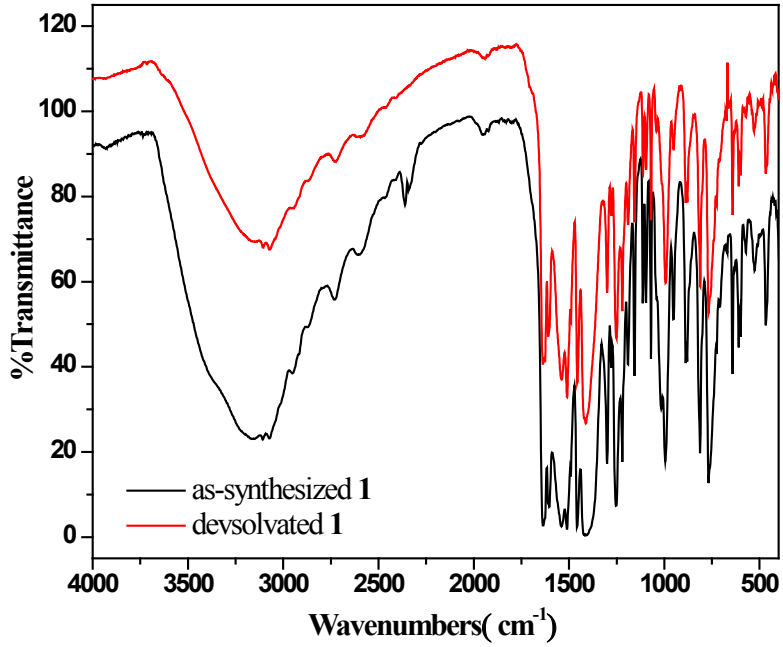

(a)

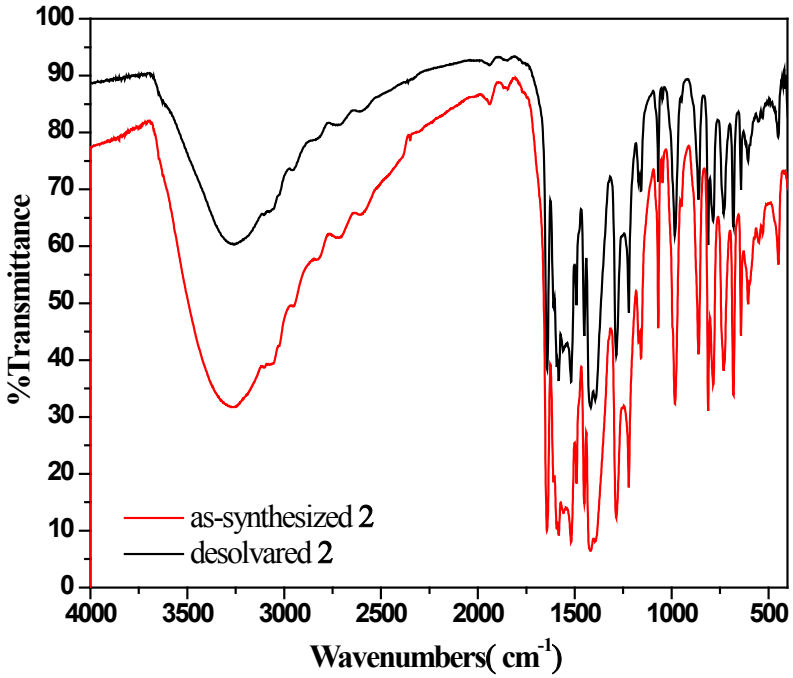

(b)

Figure S7. IR spectra for (a) as-synthesized **1** and desolvated-**1**, and (b) as-synthesized **2** and desolvated-**2**.

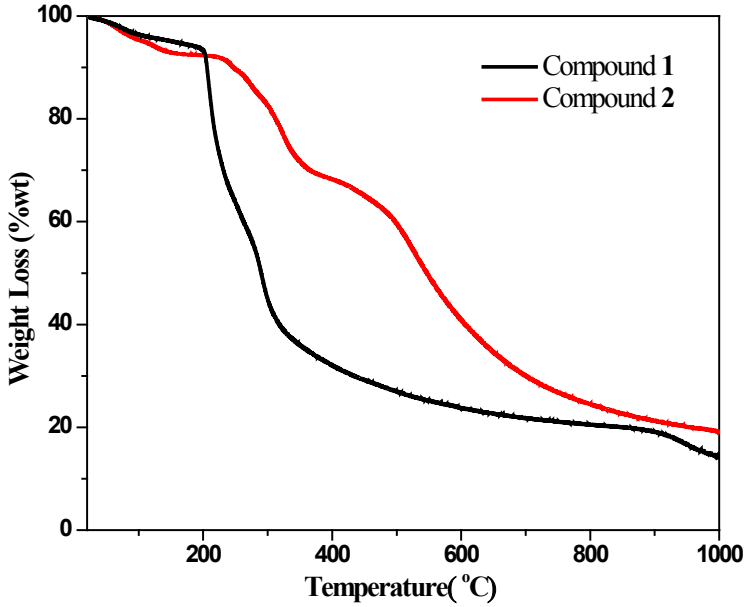

Figure S8. TG curves for compounds **1** and **2**.

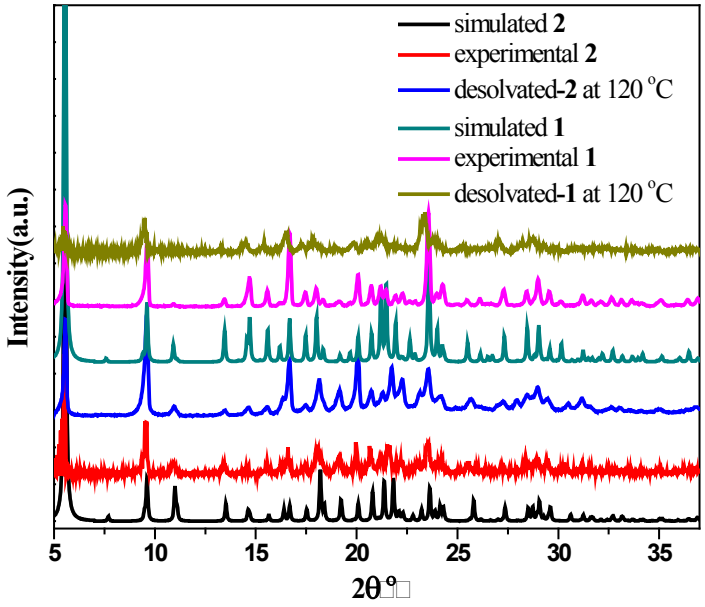

Figure S9. Powder XRD profiles of simulated **1**, experimental **1**, desolvated-**1**, simulated **2**, experimental **2** and desolvated-**2**.

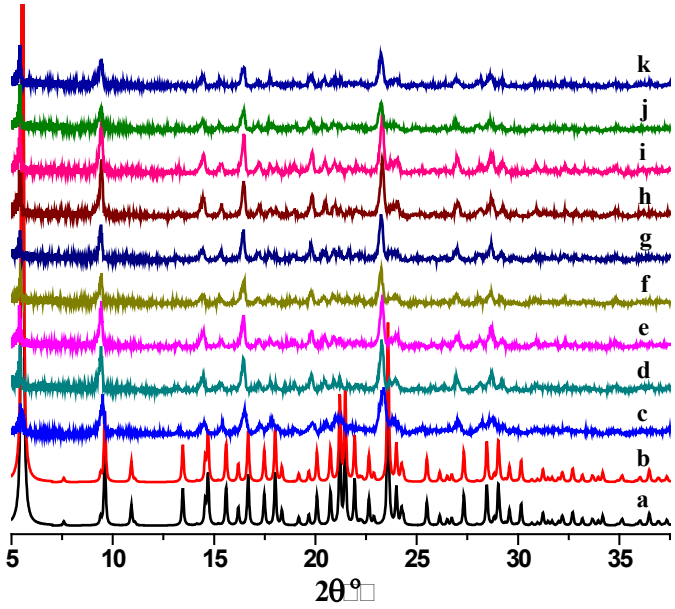

Figure S10. Powder XRD profiles of (a) simulated **1**, (b) experimental **1**, (c) desolvated-**1** for fluorescence examination and desolvated-**1** immersed in different solvents for 2 days: (d) acetone, (e) cyclohexane, (f) EtOH, (g) THF, (h) CH_2Cl_2, (i) CH_3CN, (j) CH_3OH, and (k) H_2O.

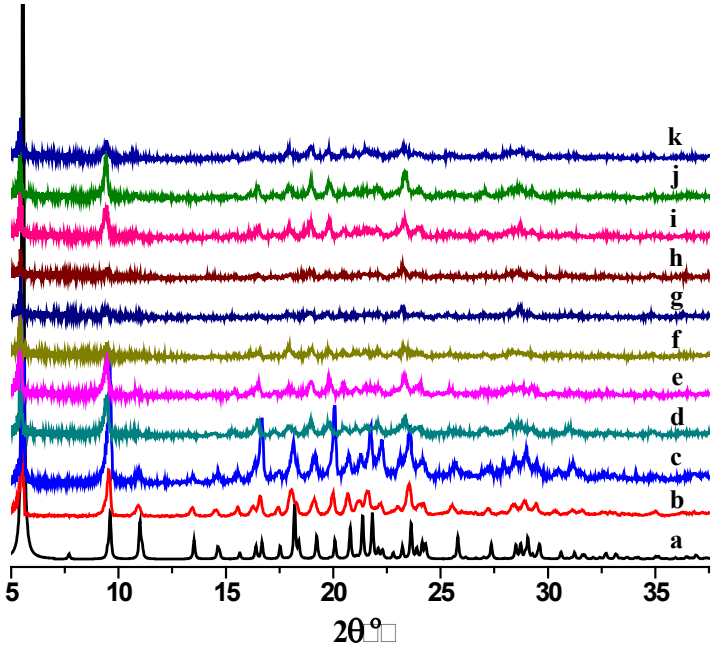

Figure S11. Powder XRD profiles of (a) simulated **2**, (b) experimental **2**, (c) desolvated-**2** for fluorescence examination and desolvated-**2** immersed in different solvents for 2 days: (d) CH_3CN, (e) THF, (f) CH_3OH, (g) EtOH, (h) acetone, (i) CH_2Cl_2, (j) cyclohexane, and (k) H_2O.

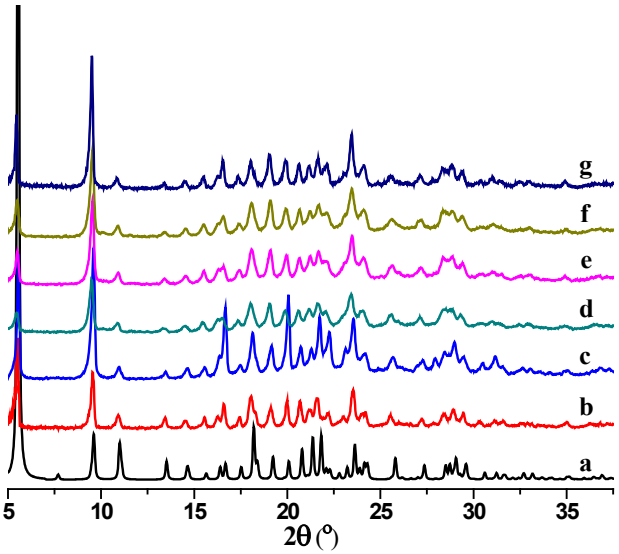

Figure S12. Powder XRD profiles of (a) simulated **2**, (b) experimental **2**, (c) desolvated-**2** for solid-state fluorescence examination and desolvated-**2** immersed in different solvents for 2 days: (d) C_6H_6 (benzene), (e) $C_6H_6CH_3$ (toluene), (f) C_6H_6I (iodobenzene), and (g) $C_6H_6NO_2$ (nitrobenzene).

Section 8. UV-vis and PL spectra of 1 and 2.

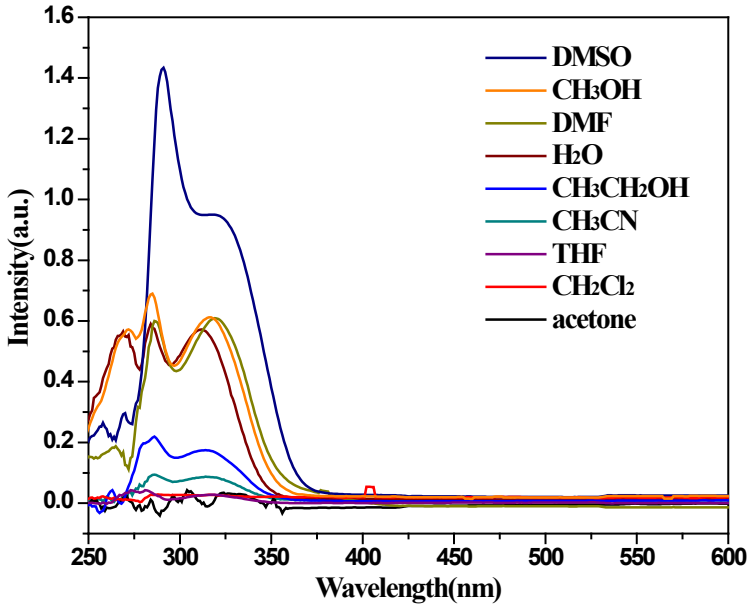

Figure S13. UV-vis spectra of compound **1** introduced into various pure solvents.

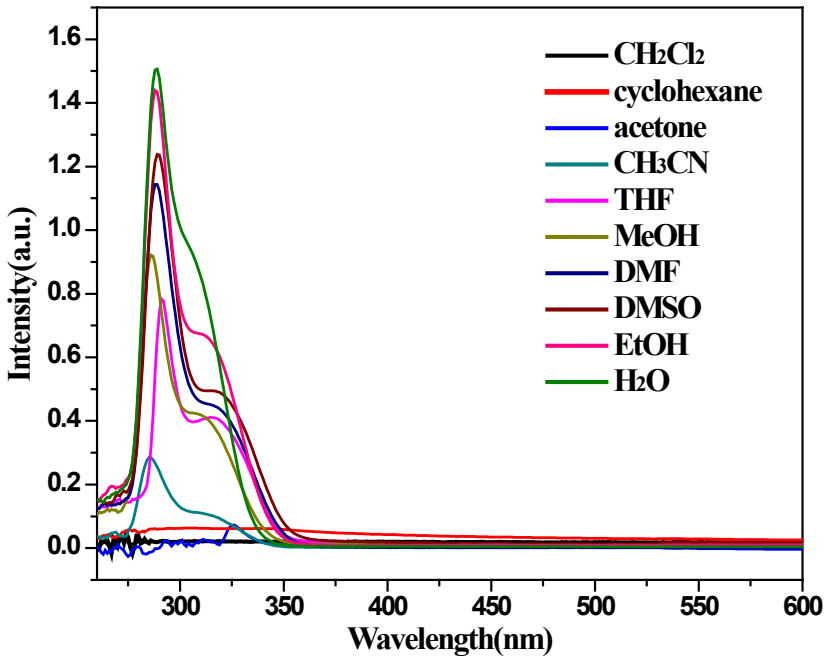

Figure S14. UV-vis spectra of compound **2** introduced into various pure solvents.

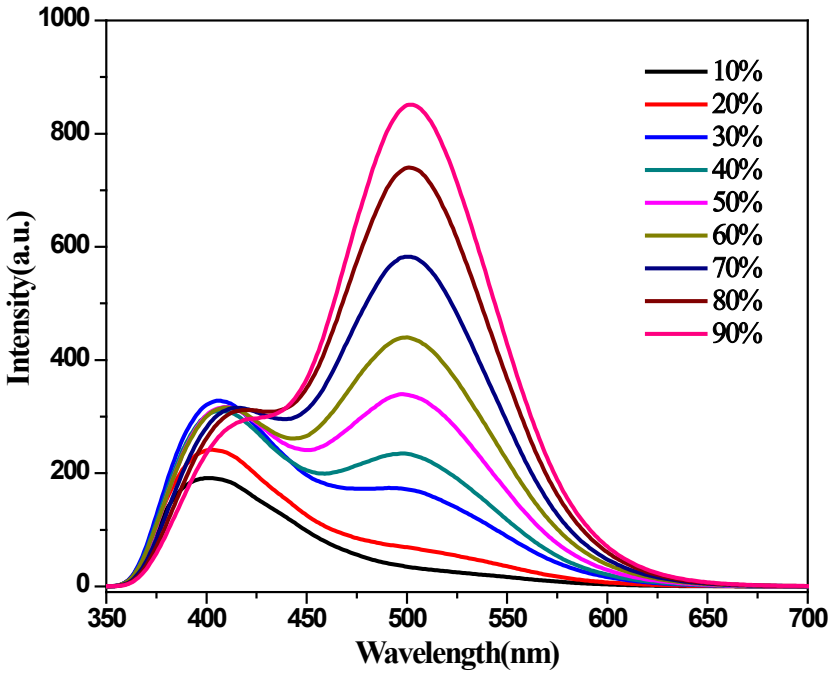

Figure S15. The PL spectra of **1a** methanol emulsion in the presence of various amounts of H_2O under λ_{ex} = 286 nm.

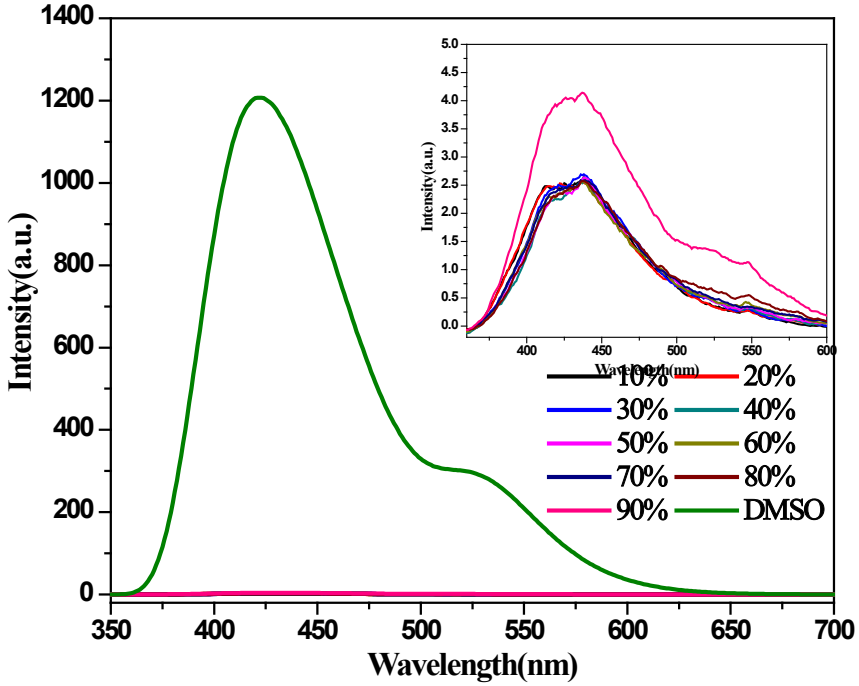

Figure S16. The PL spectra of **1a** DMSO solution and **1a** acetone emulsion in the presence of various amounts of DMSO under λ_{ex} = 286 nm.

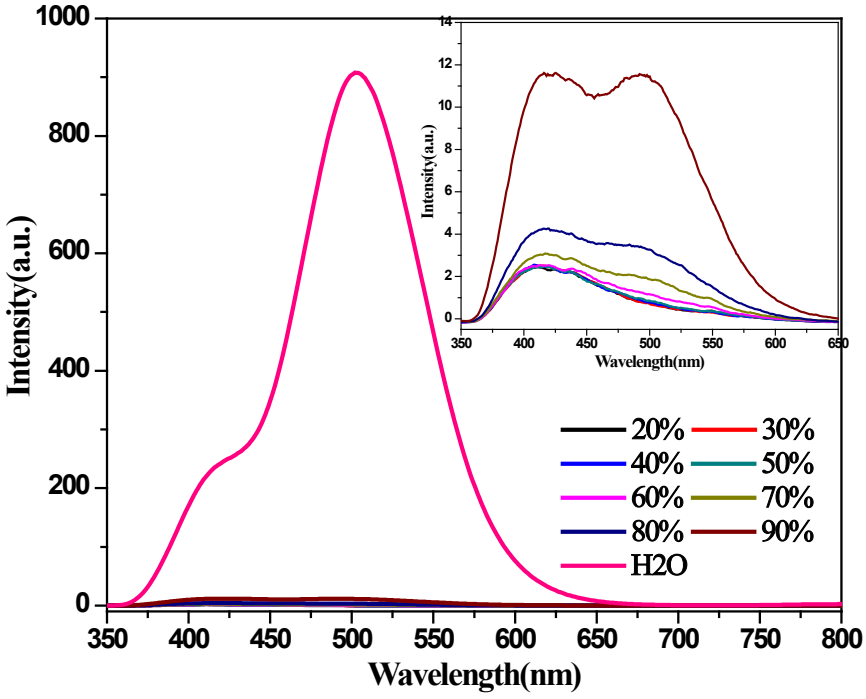

Figure S17. The PL spectra of **1a** H_2O solution and **1a** acetone emulsion in the presence of various amounts of H_2O under λ_{ex} = 286 nm.

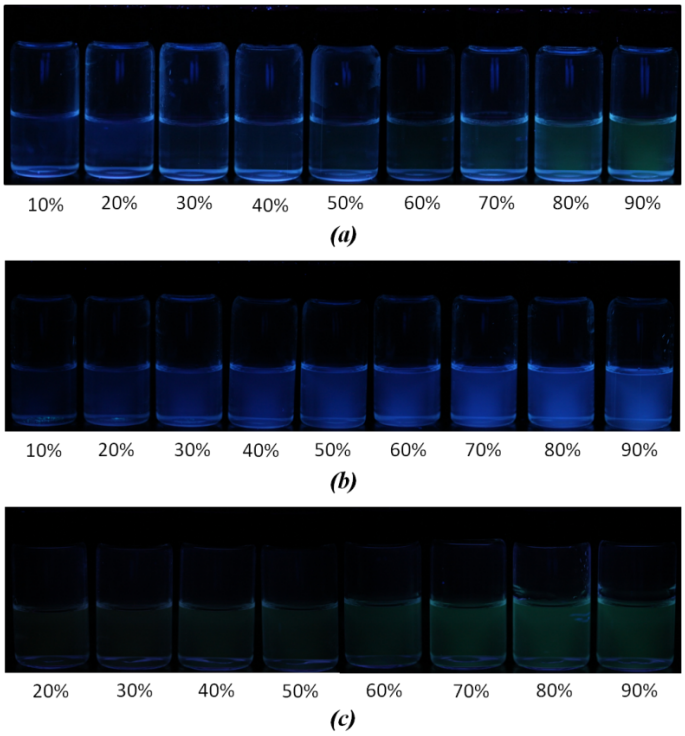

Figure S18. Photographs of fluorescence emission of **1a** taken during PL spectra collection in different solvents for sensing properties with respect to (a) H_2O and methanol, (b) DMSO and acetone, and (c) H_2O and acetone.

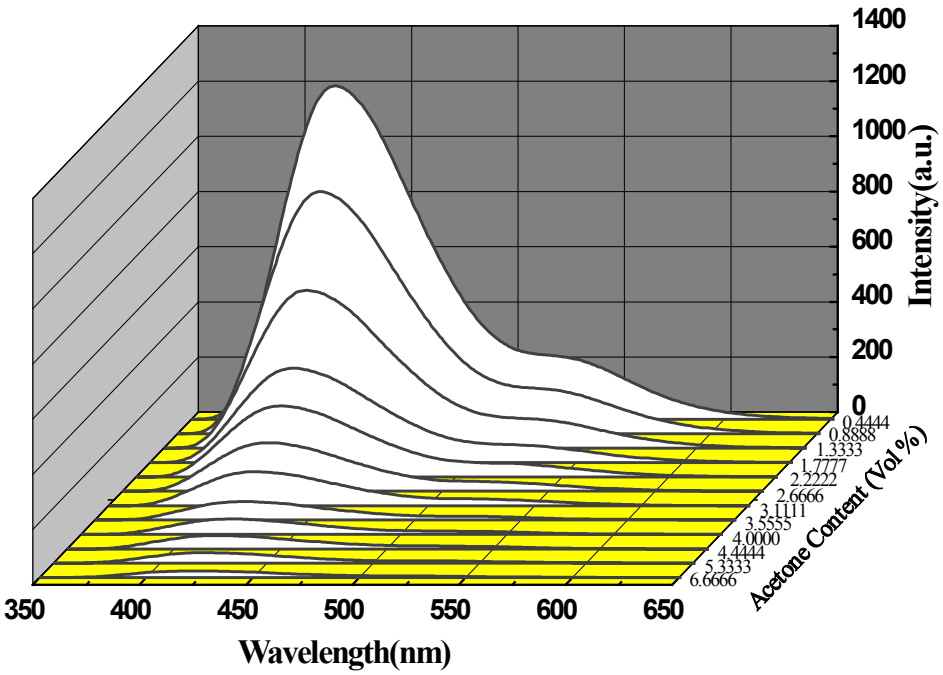

Figure S19. The PL spectra of **1a** DMSO solution in the presence of various amounts of acetone under λ_{ex} = 286 nm.

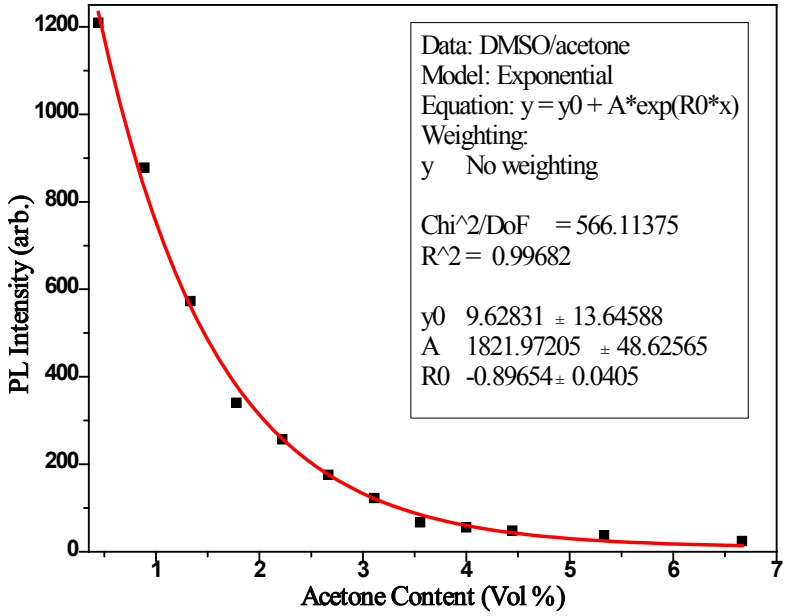

Figure S20. The PL intensity of **1a** DMSO solution as a function of acetone content.

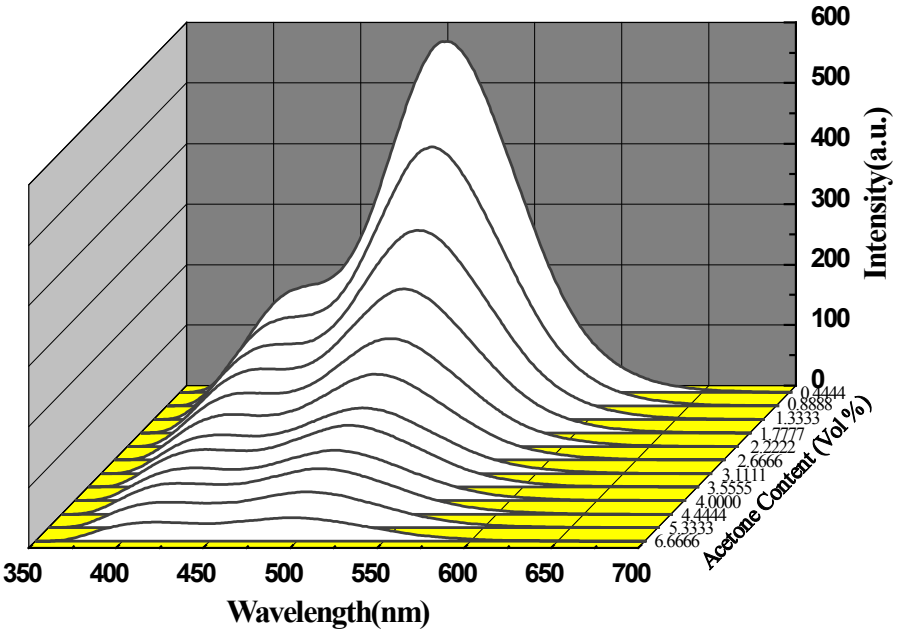

Figure S21. The PL spectra of **1a** H_2O emulsion in the presence of various amounts of acetone under λ_{ex} = 286 nm.

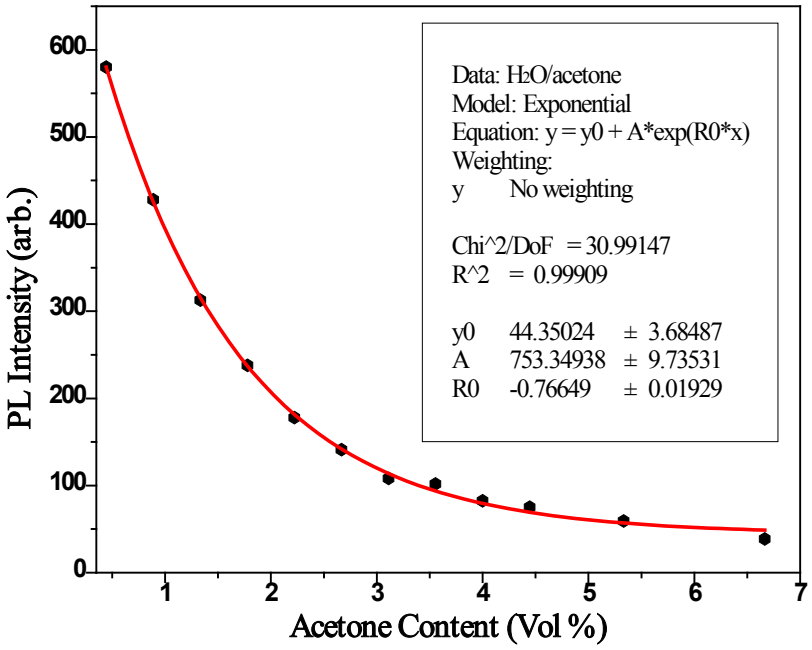

Figure S22. The PL intensity of **1a** H_2O solution as a function of acetone content.

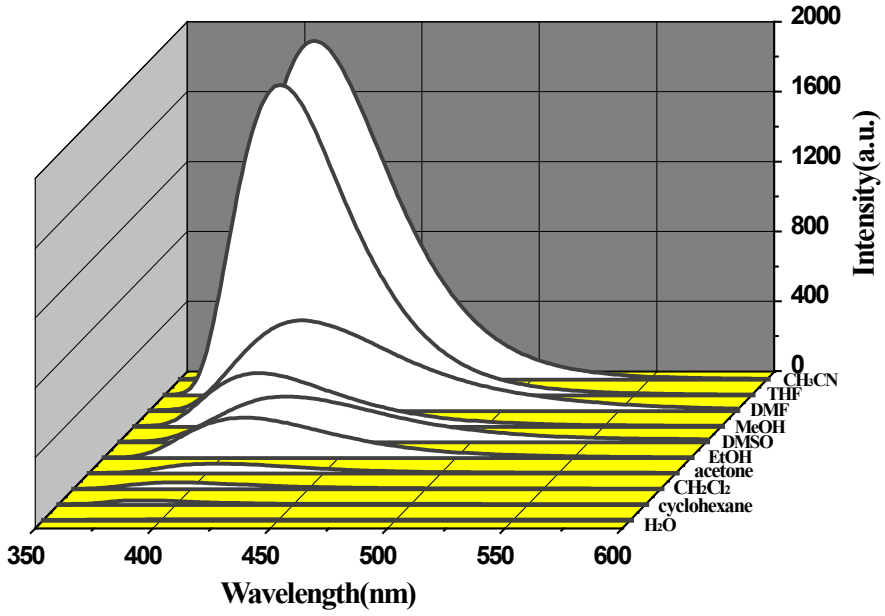

Figure S23. Fluorescence spectra of desolvated-**2** (**2a**) introduced into various pure solvents when excited at 286 nm.

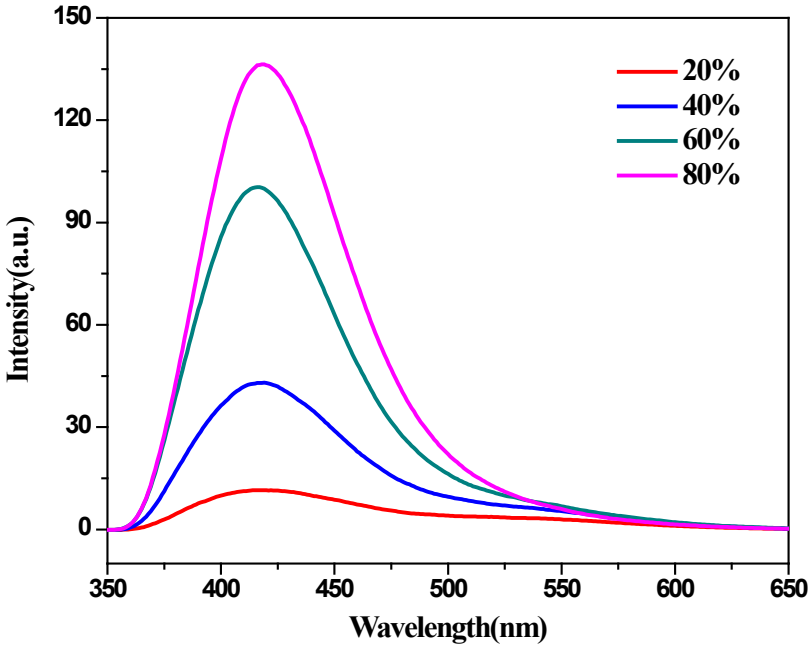

Figure S24. PL spectra of **2a** water emulsion in the presence of various amounts of CH_3CN under λ_{ex} = 286 nm.

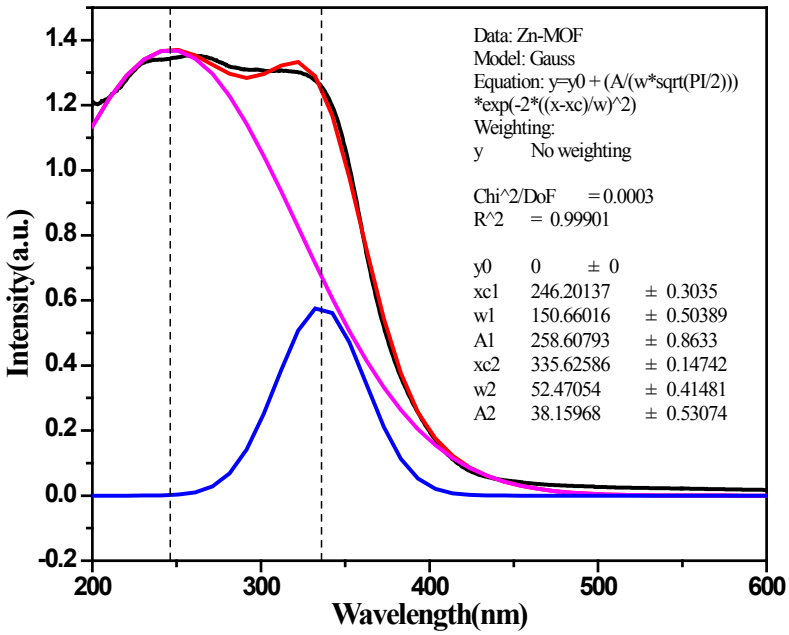

Figure S25. Solid-state UV-vis spectra of compound **2**.

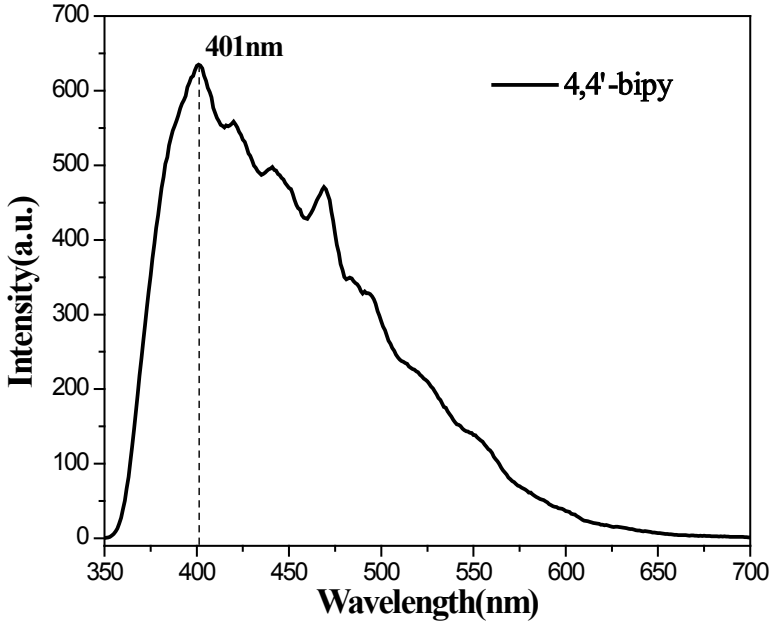

Figure S26. Solid-state fluorescence spectra picture of 4,4'-bipy.

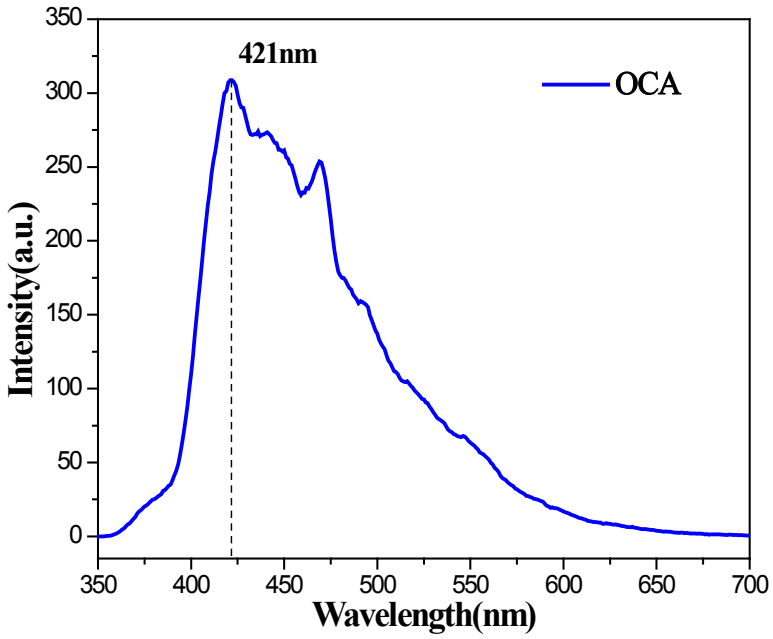

Figure S27. Solid-state fluorescence spectra picture of OCA-OH.

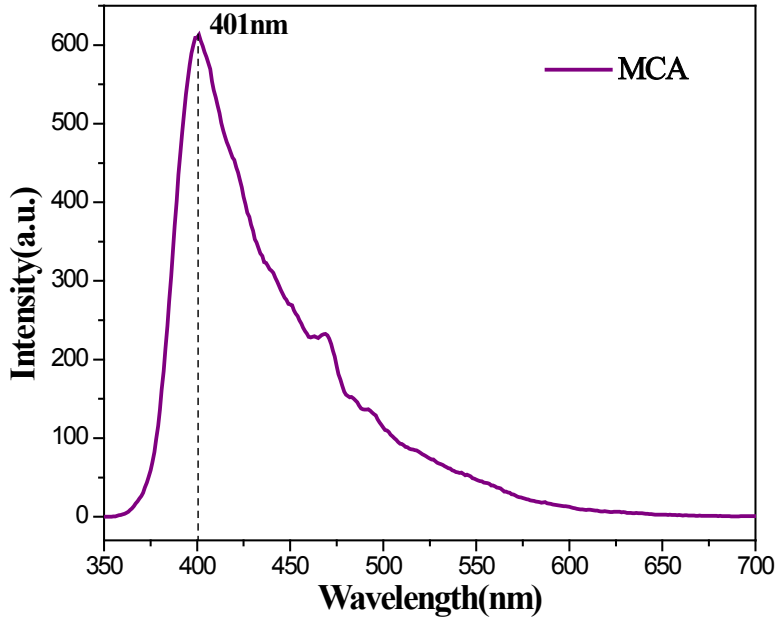

Figure S28. Solid-state fluorescence spectra picture of MCA-OH.

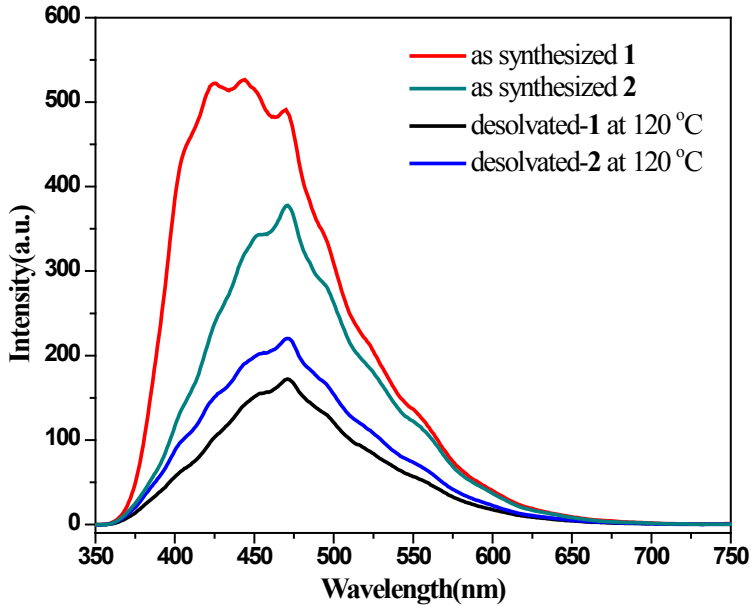

Figure S29. Solid-state fluorescence spectra pictures of compounds **1**, desolvated-**1** (**1a**), **2** and desolvated-**2** (**2a**).

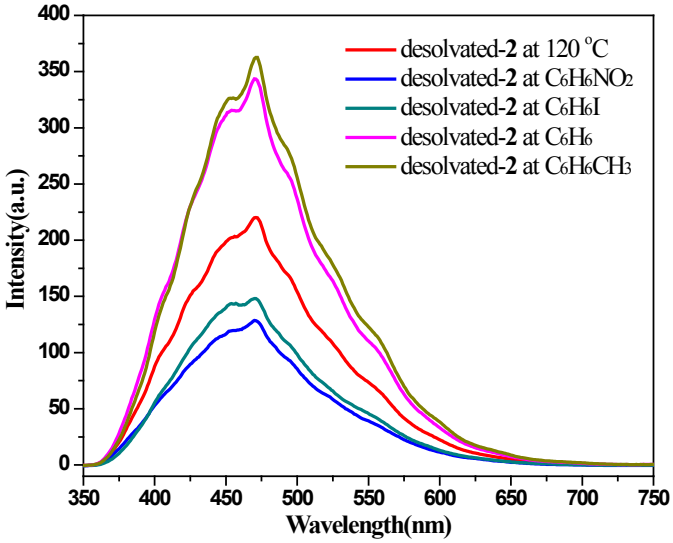

Figure S30. Solid-state fluorescence spectra pictures of desolvated-**2** (**2a**), desolvated-**2** immersed in C_6H_6 (benzene), $C_6H_6CH_3$ (toluene), C_6H_6I (iodobenzene), and $C_6H_6NO_2$ (nitrobenzene) for 2 days.

Section 9. PL spectra of ligands, ligands+metals and normalized PL spectra of ligands, ligands+metals and MOF-desolvated

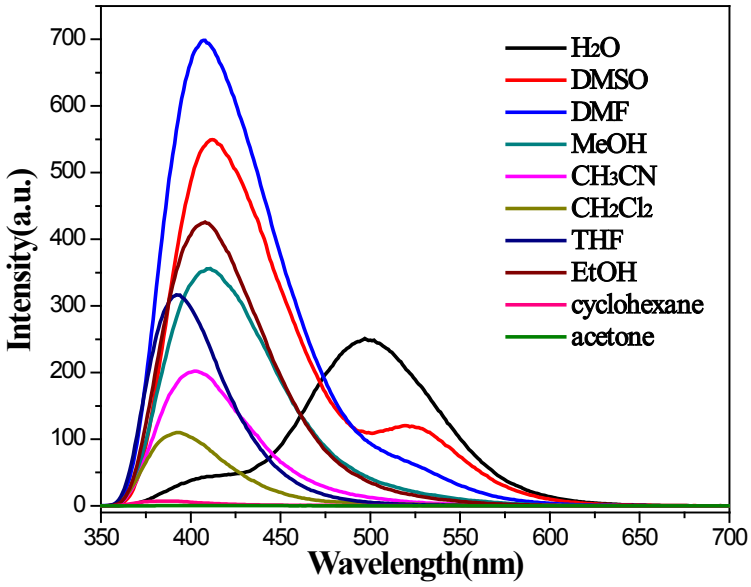

Figure S31. Emission spectra of ligands(OCA-OH and 4,4'-bipy) + metals($Zn(ClO_4)_2 \cdot 6H_2O$) introduced into various pure solvents (4×10^{-5} mol·L^{-1}) when excited at 286 nm.

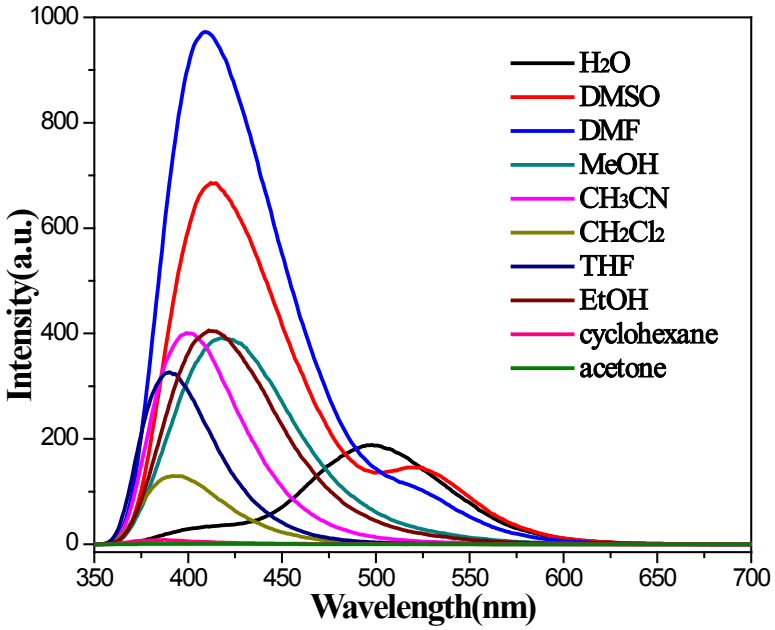

Figure S32. Emission spectra of ligands (OCA-OH and 4,4'-bipy) introduced into various pure solvents (4×10^{-5} mol·L^{-1}) when excited at 286 nm.

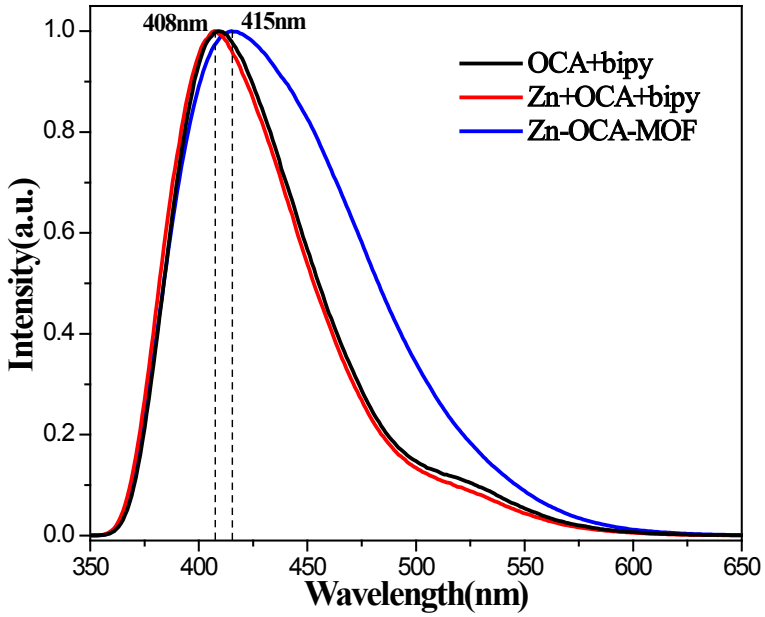

Figure S33. Normalized emission spectra of lagands(OCA-OH and 4,4'-bipy), ligands(OCA-OH and 4,4'-bipy)＋metals ($Zn(ClO_4)_2\cdot6H_2O$) and desolvated-**1** (**1a**) introduced into DMF pure solvent(4×10^{-5} mol·L^{-1}) when excited at 286 nm.

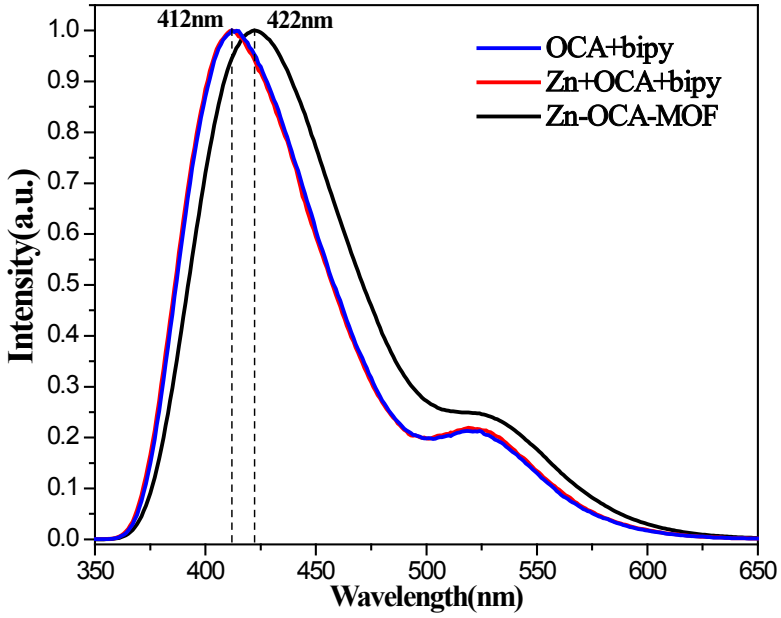

Figure S34. Normalized emission spectra of lagands(OCA-OH and 4,4'-bipy), ligands(OCA-OH and 4,4'-bipy)＋metals ($Zn(ClO_4)_2 \cdot 6H_2O$) and desolvated-**1** (**1a**) introduced into DMSO pure solvent(4×10^{-5} mol·L^{-1}) when excited at 286 nm.

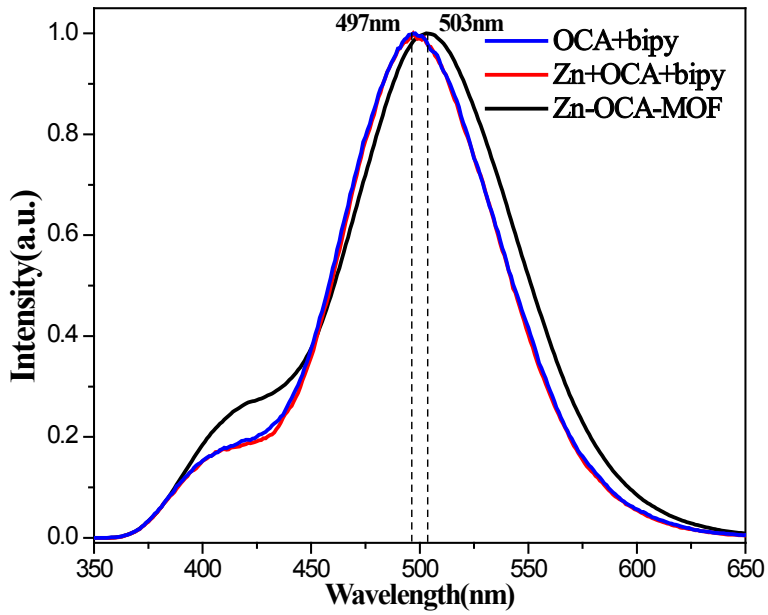

Figure S35. Normalized emission spectra of lagands(OCA-OH and 4,4'-bipy), ligands(OCA-OH and 4,4'-bipy)＋metals ($Zn(ClO_4)_2 \cdot 6H_2O$) and desolvated-**1** (**1a**) introduced into H_2O pure

solvent(4×10^{-5} mol·L^{-1}) when excited at 286 nm.

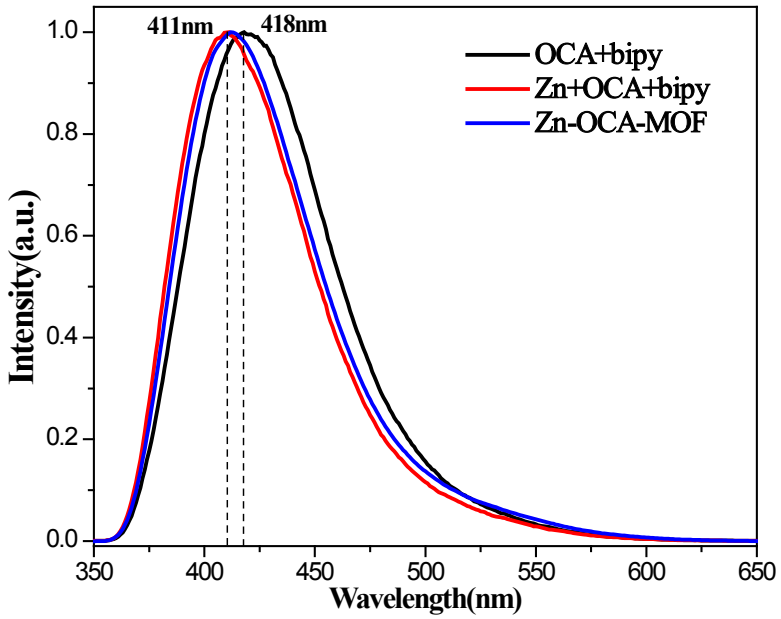

Figure S36. Normalized emission spectra of lagands(OCA-OH and 4,4'-bipy), ligands(OCA-OH and 4,4'-bipy)＋metals ($Zn(ClO_4)_2\cdot6H_2O$) and desolvated-**1** (**1a**) introduced into MeOH pure solvent(4×10^{-5} mol·L^{-1}) when excited at 286 nm.

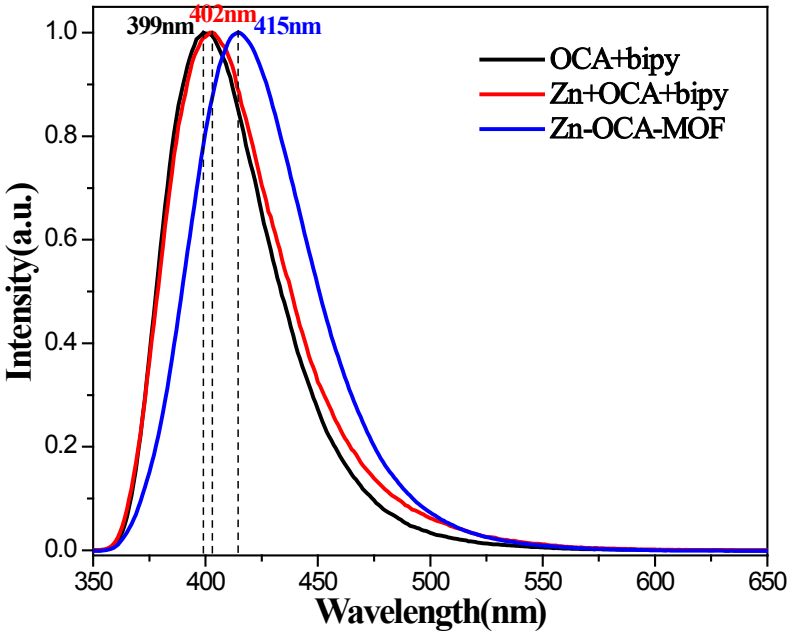

Figure S37. Normalized emission spectra of lagands(OCA-OH and 4,4'-bipy), ligands(OCA-OH

and 4,4'-bipy)＋metals ($Zn(ClO_4)_2 \cdot 6H_2O$) and desolvated-**1** (**1a**) introduced into CH_3CN pure solvent(4×10^{-5} mol·L^{-1}) when excited at 286 nm.

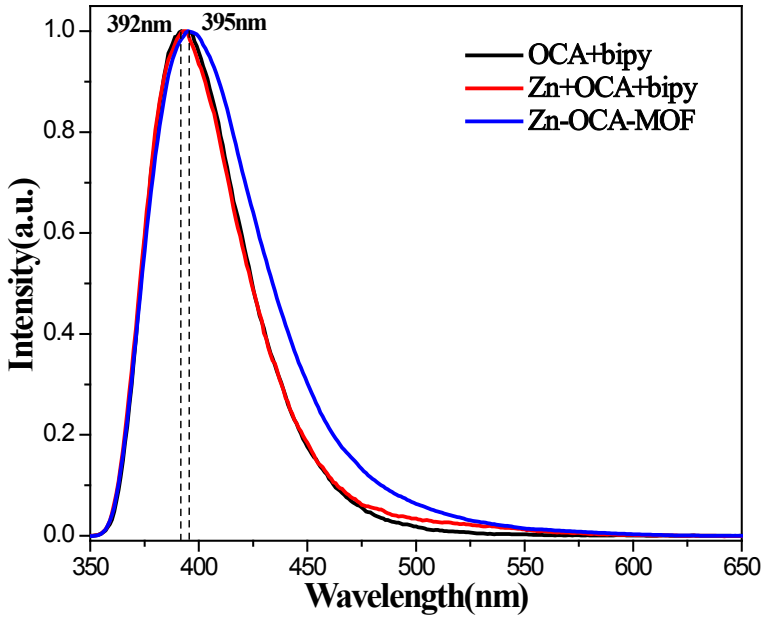

Figure S38. Normalized emission spectra of lagands(OCA-OH and 4,4'-bipy), ligands(OCA-OH and 4,4'-bipy)＋metals ($Zn(ClO_4)_2 \cdot 6H_2O$) and desolvated-**1** (**1a**) introduced into CH_2Cl_2 pure solvent(4×10^{-5} mol·L^{-1}) when excited at 286 nm.

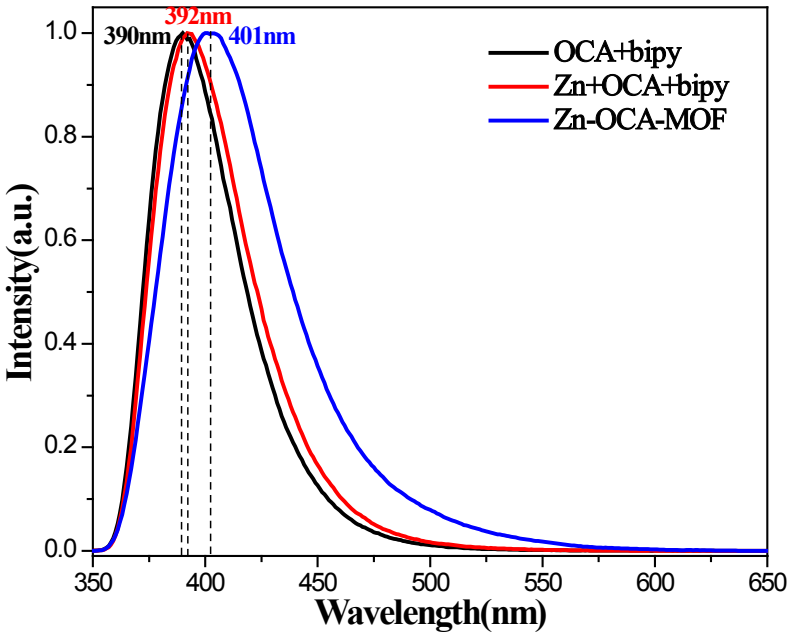

Figure S39. Normalized emission spectra of lagands(OCA-OH and 4,4'-bipy), ligands(OCA-OH and 4,4'-bipy)＋metals ($Zn(ClO_4)_2 \cdot 6H_2O$) and desolvated-**1** (**1a**) introduced into THF pure solvent(4×10^{-5} mol·L^{-1}) when excited at 286 nm.

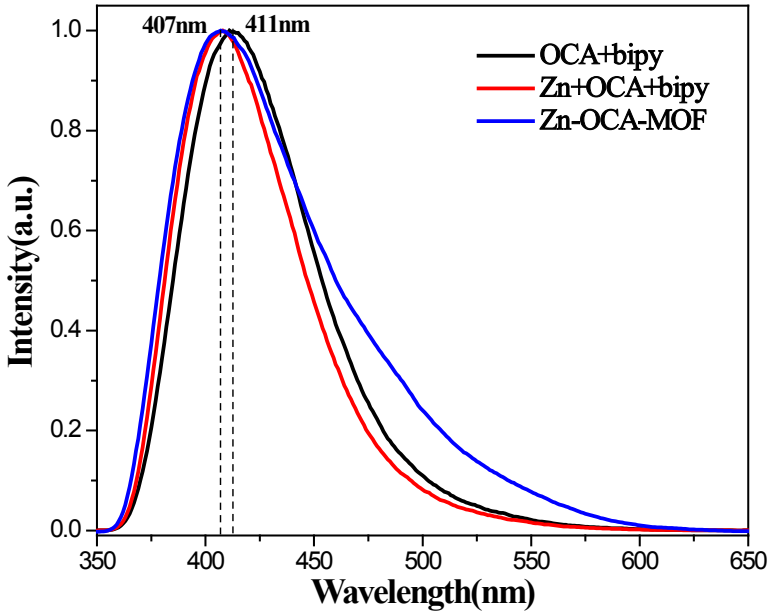

Figure S40. Normalized emission spectra of lagands(OCA-OH and 4,4'-bipy), ligands(OCA-OH and 4,4'-bipy)＋metals ($Zn(ClO_4)_2 \cdot 6H_2O$) and desolvated-**1** (**1a**) introduced into EtOH pure solvent(4×10^{-5} mol·L^{-1}) when excited at 286 nm.

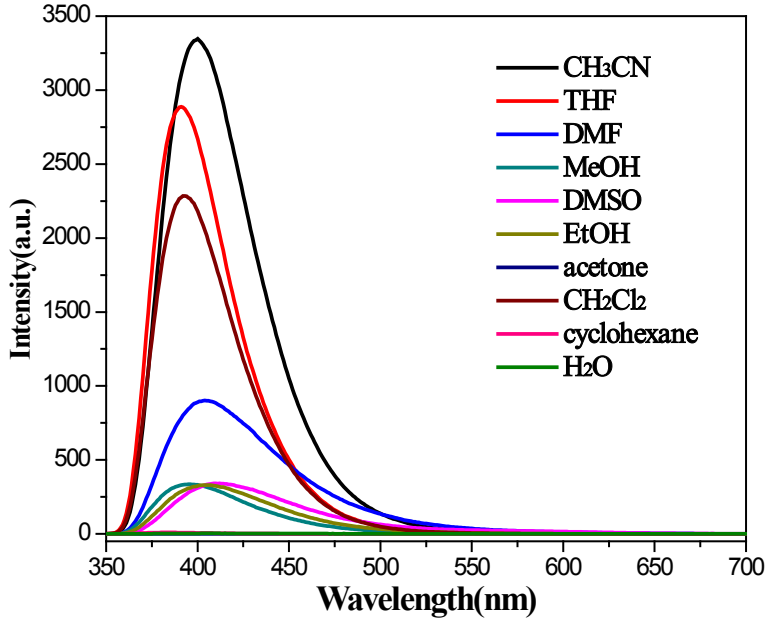

Figure S41. Emission spectra of ligands(MCA-OH and 4,4'-bipy) + metals($Zn(ClO_4)_2 \cdot 6H_2O$) introduced into various pure solvents (4×10^{-5} mol·L^{-1}) when excited at 286 nm.

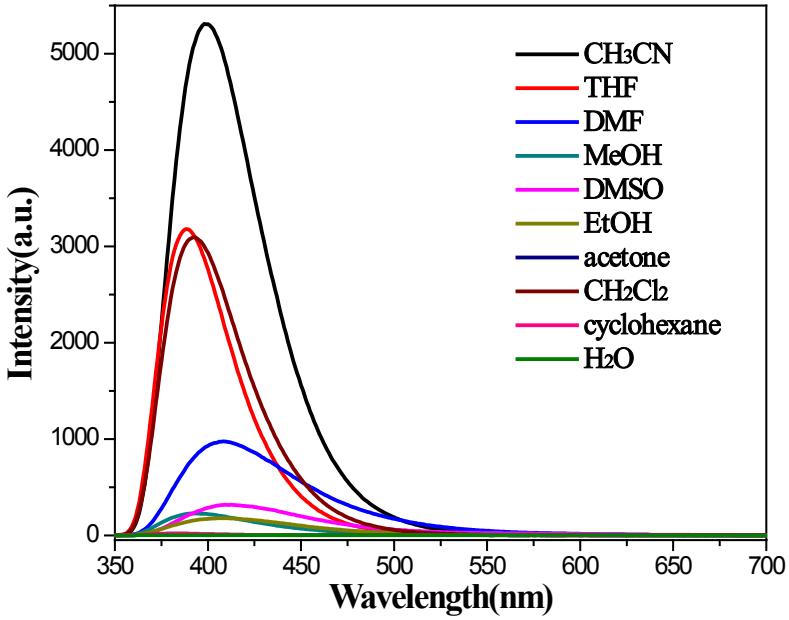

Figure S42. Emission spectra of ligands (MCA-OH and 4,4'-bipy) introduced into various pure solvents (4×10^{-5} mol·L^{-1}) when excited at 286 nm.

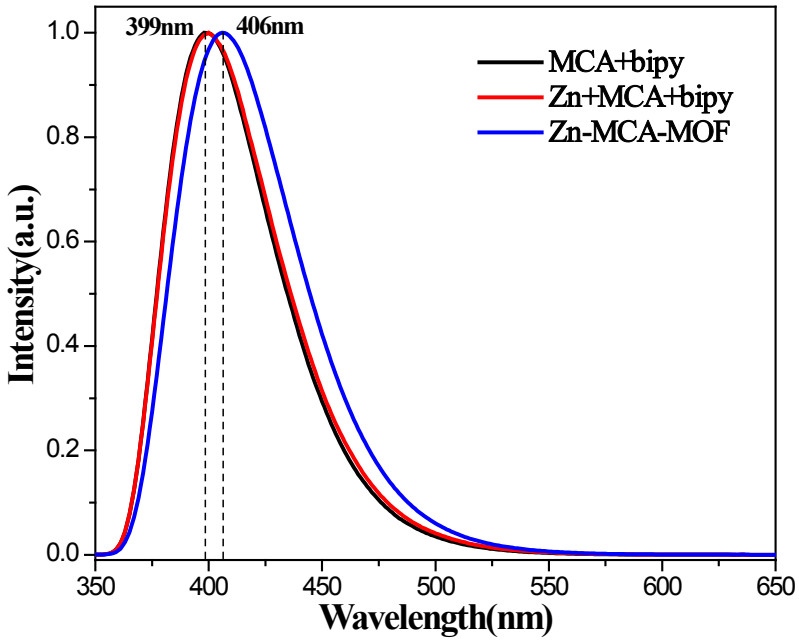

Figure S43. Normalized emission spectra of lagands(MCA-OH and 4,4'-bipy), ligands(MCA-OH

and 4,4'-bipy)＋metals ($Zn(ClO_4)_2 \cdot 6H_2O$) and desolvated-**2** (**2a**) introduced into CH_3CN pure solvent(4×10^{-5} mol·L^{-1}) when excited at 286 nm.

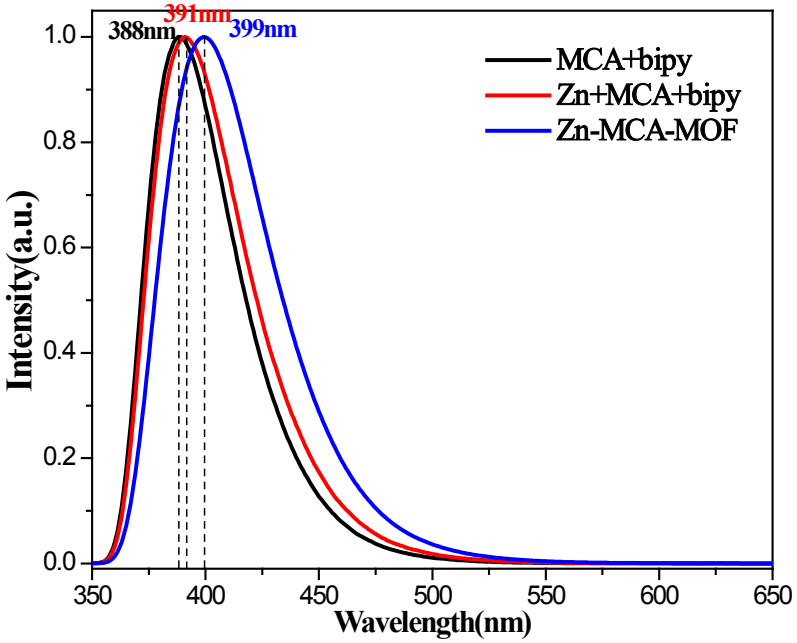

Figure S44. Normalized emission spectra of lagands(MCA-OH and 4,4'-bipy), ligands(MCA-OH and 4,4'-bipy)＋metals ($Zn(ClO_4)_2 \cdot 6H_2O$) and desolvated-**2** (**2a**) introduced into THF pure solvent(4×10^{-5} mol·L^{-1}) when excited at 286 nm.

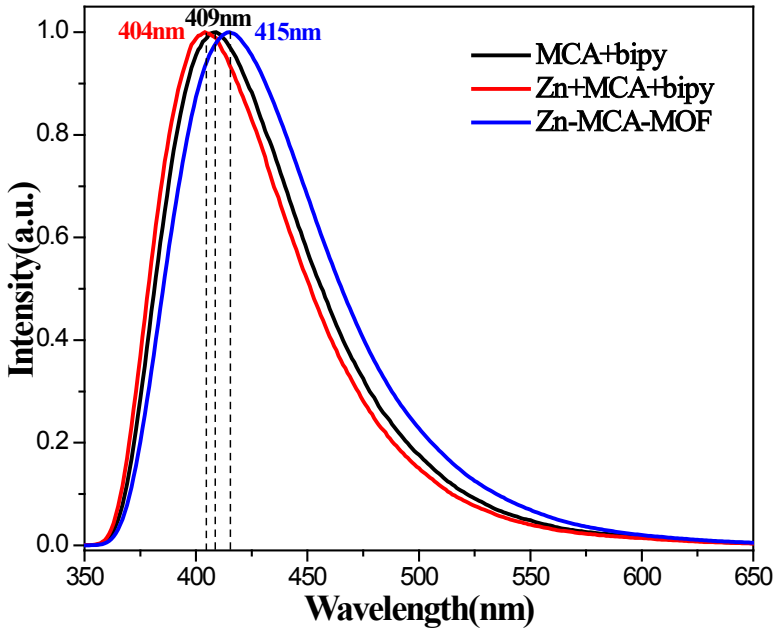

Figure S45. Emission spectra of lagands(MCA-OH and 4,4'-bipy), ligands(MCA-OH and 4,4'-bipy) + metals ($Zn(ClO_4)_2 \cdot 6H_2O$) and desolvated-**2** (**2a**) introduced into DMF pure solvent(4×10^{-5} mol·L^{-1}) when excited at 286 nm.

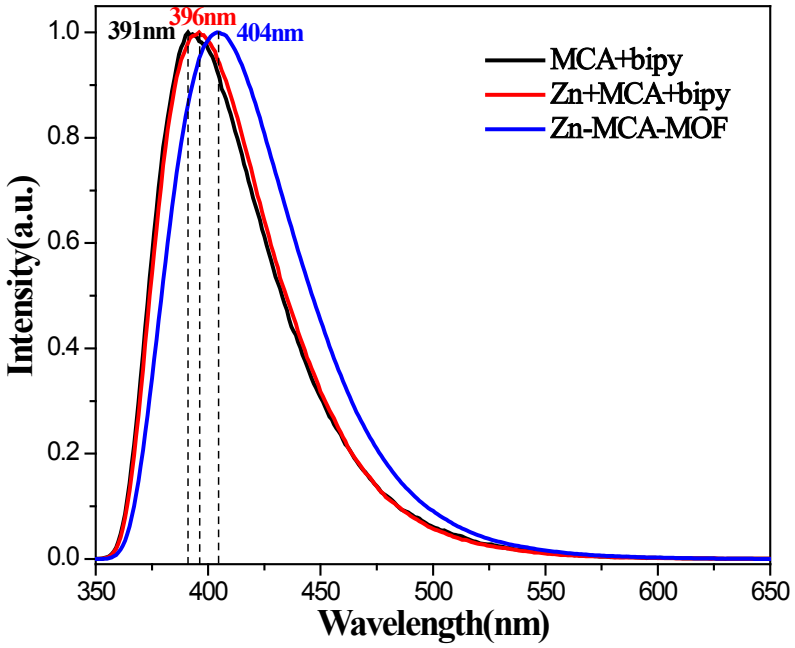

Figure S46. Emission spectra of lagands(MCA-OH and 4,4'-bipy), ligands(MCA-OH and 4,4'-bipy) + metals ($Zn(ClO_4)_2 \cdot 6H_2O$) and desolvated-**2** (**2a**) introduced into MeOH pure solvent(4×10^{-5} mol·L^{-1}) when excited at 286 nm.

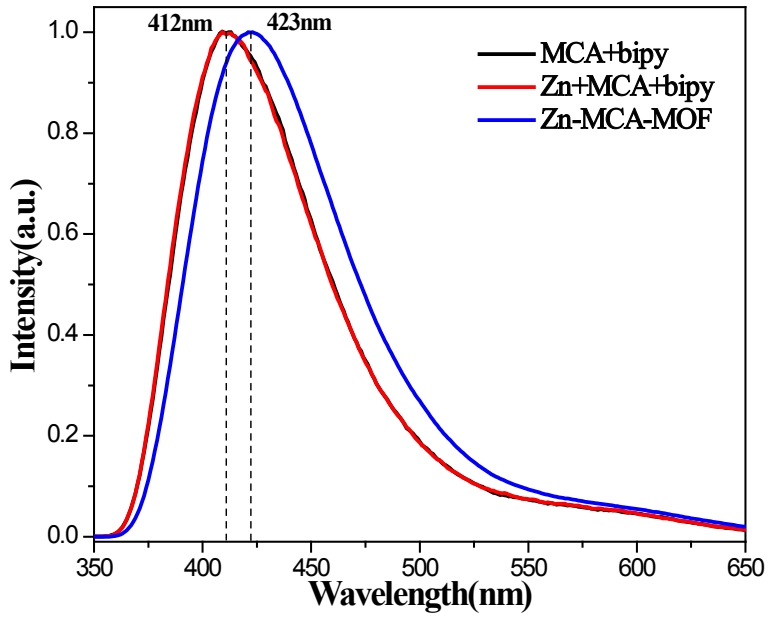

Figure S47. Emission spectra of lagands(MCA-OH and 4,4'-bipy), ligands(MCA-OH and 4,4'-bipy) + metals ($Zn(ClO_4)_2 \cdot 6H_2O$) and desolvated-**2** (**2a**) introduced into DMSO pure solvent(4×10^{-5} mol·L^{-1}) when excited at 286 nm.

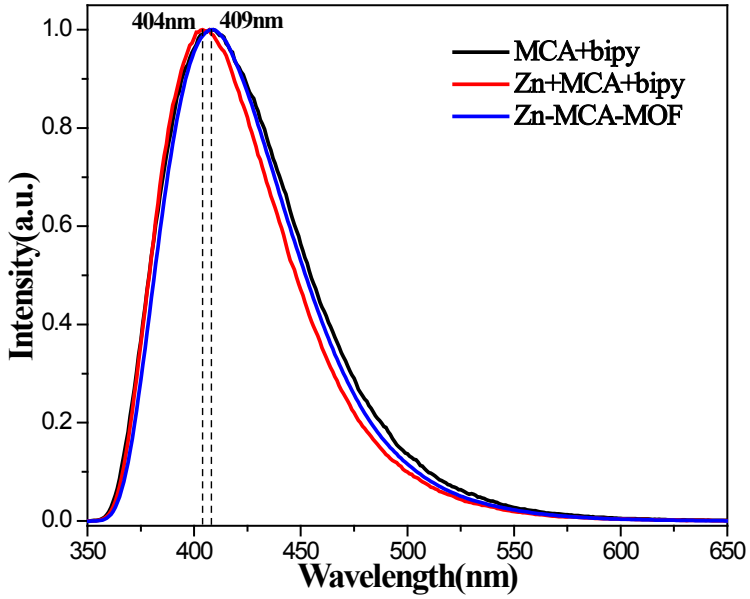

Figure S48. Emission spectra of lagands(MCA-OH and 4,4'-bipy), ligands(MCA-OH and 4,4'-bipy) + metals ($Zn(ClO_4)_2 \cdot 6H_2O$) and desolvated-**2** (**2a**) introduced into EtOH pure solvent(4×10^{-5} mol·L^{-1}) when excited at 286 nm.

Section 10. TGA Curves of 1⊃Solvents and 2⊃Solvents

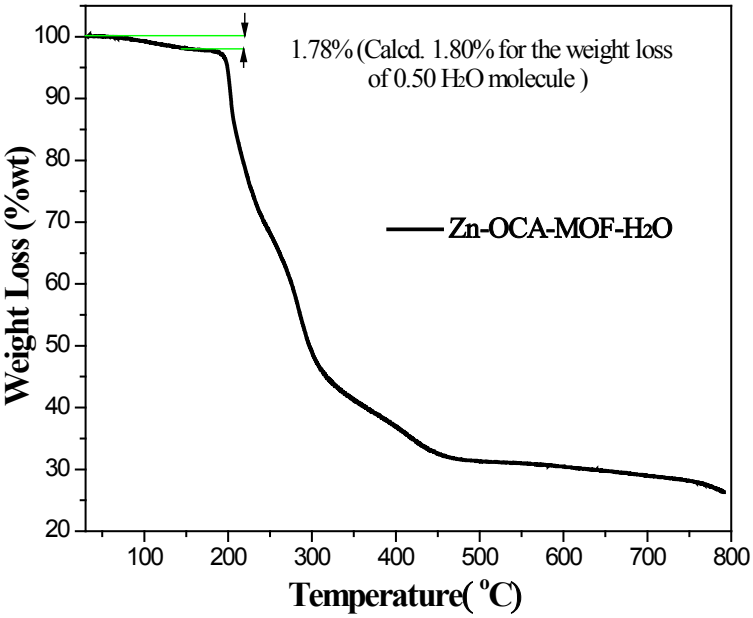

Figure S49. TG analysis of H_2O adsorbed form, 1⊃H_2O. The observed weight loss (1.78%) is the weight of 0.50 H_2O molecules.

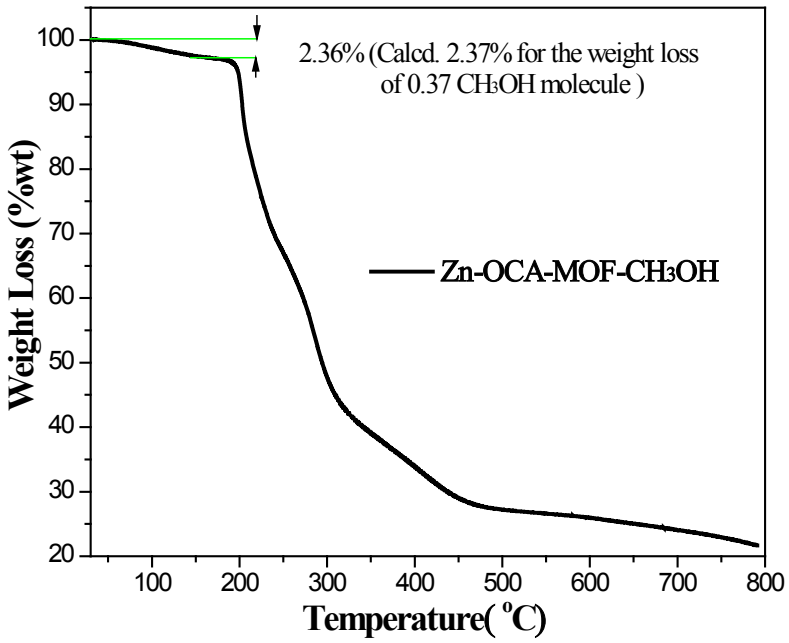

Figure S50. TG analysis of CH_3OH adsorbed form, 1⊃CH_3OH. The observed weight loss (2.36%) is the weight of 0.37 CH_3OH molecules.

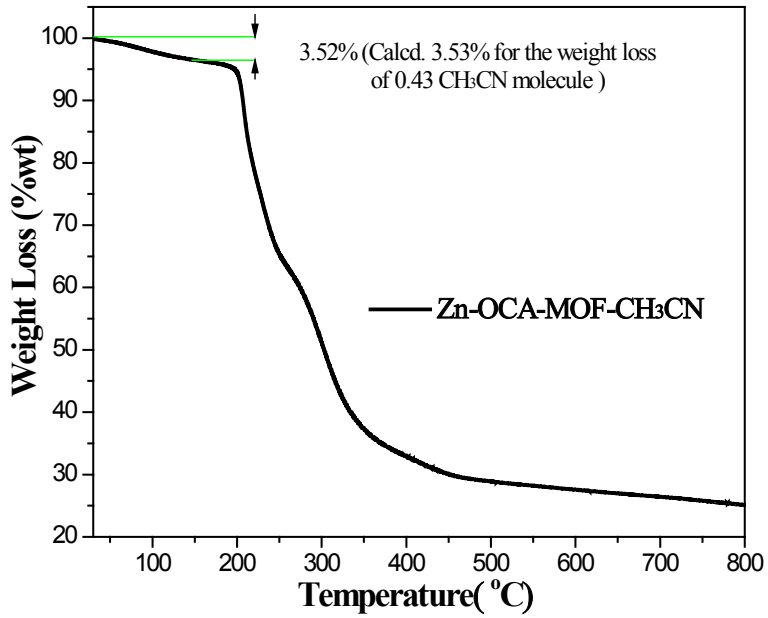

Figure S51. TG analysis of CH_3CN adsorbed form, 1⊃CH_3CN. The observed weight loss (3.52%) is the weight of 0.43 CH_3CN molecules.

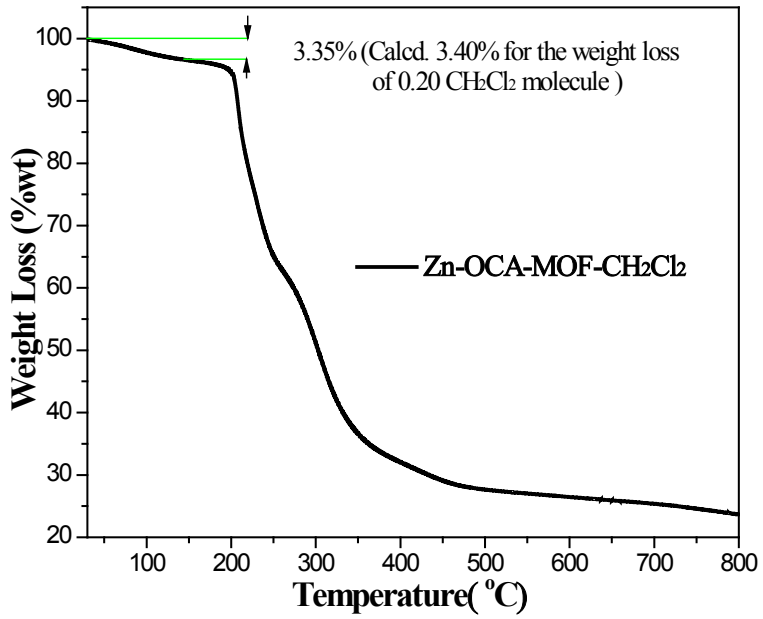

Figure S52. TG analysis of CH_2Cl_2 adsorbed form, $1 \supset CH_2Cl_2$. The observed weight loss (3.35%) is the weight of 0.20 CH_2Cl_2 molecules.

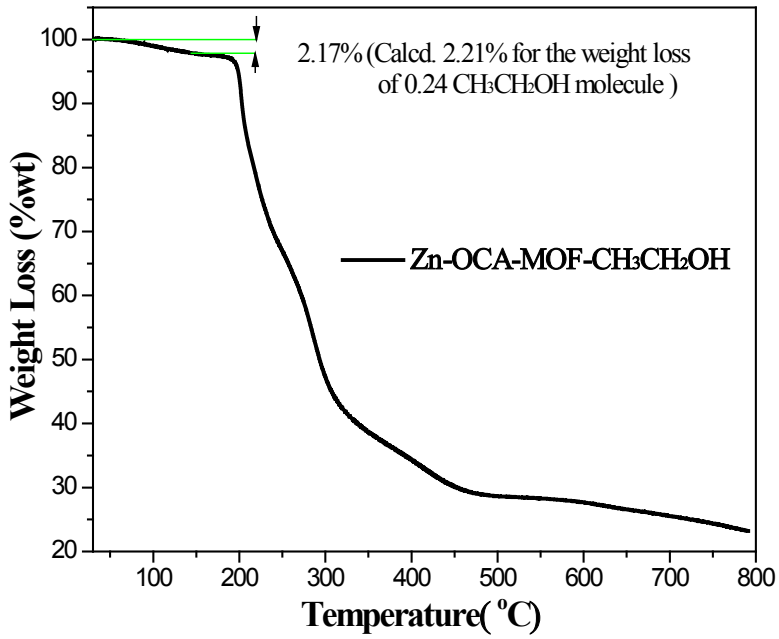

Figure S53. TG analysis of CH_3CH_2OH adsorbed form, $1 \supset CH_3CH_2OH$. The observed weight loss (2.17%) is the weight of 0.24 CH_3CH_2OH molecules.

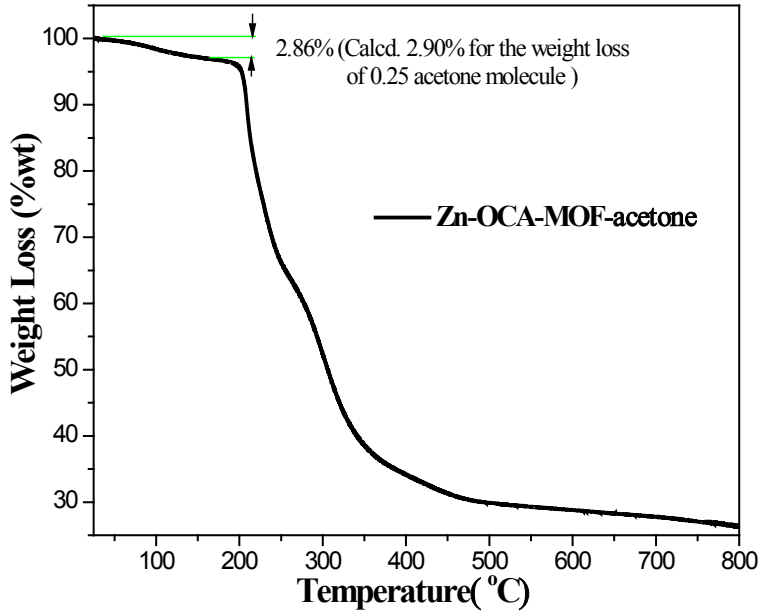

Figure S54. TG analysis of acetone adsorbed form, 1⊃acetone. The observed weight loss (2.86%) is the weight of 0.25 acetone molecules.

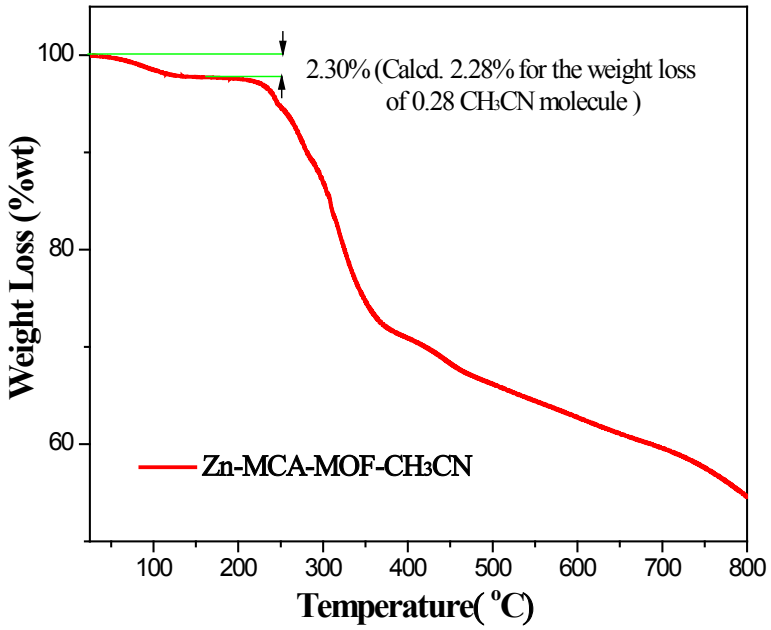

Figure S55. TG analysis of CH_3CN adsorbed form, 2⊃CH_3CN. The observed weight loss (2.30%) is the weight of 0.28 CH_3CN molecules.

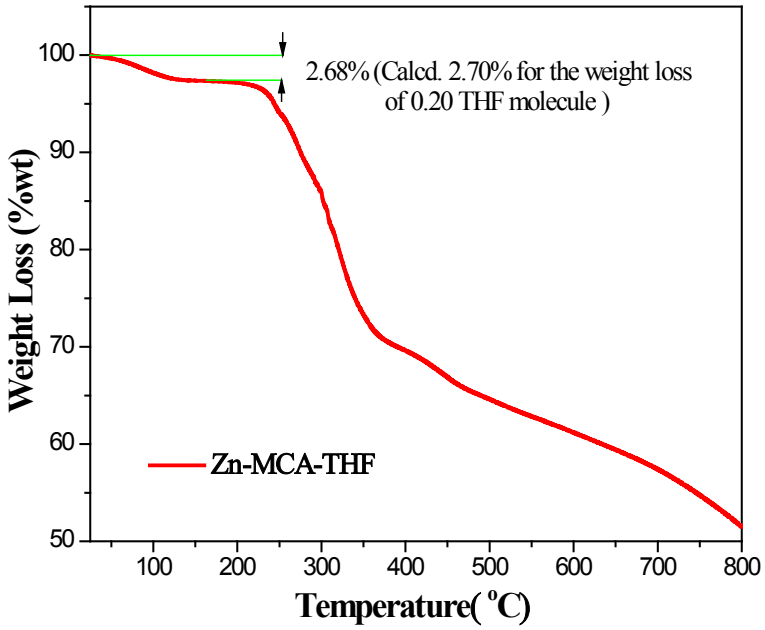

Figure S56. TG analysis of THF adsorbed form, 2⊃THF. The observed weight loss (2.68%) is the weight of 0.20 THF molecules.

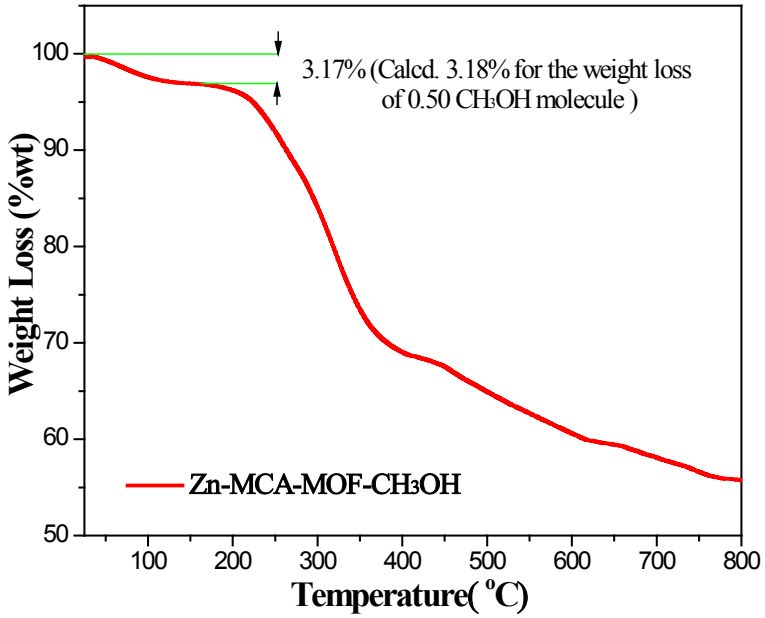

Figure S57. TG analysis of CH_3OH adsorbed form, 2⊃CH_3OH. The observed weight loss (3.17%) is the weight of 0.50 CH_3OH molecules.

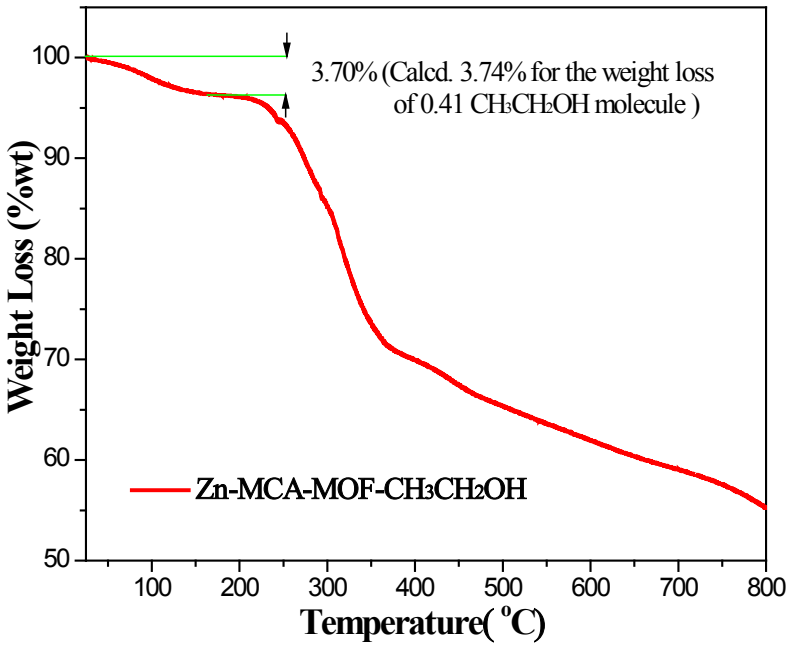

Figure S58. TG analysis of CH_3CH_2OH adsorbed form, $2\supset CH_3CH_2OH$. The observed weight loss (3.70%) is the weight of 0.41 CH_3CH_2OH molecules.

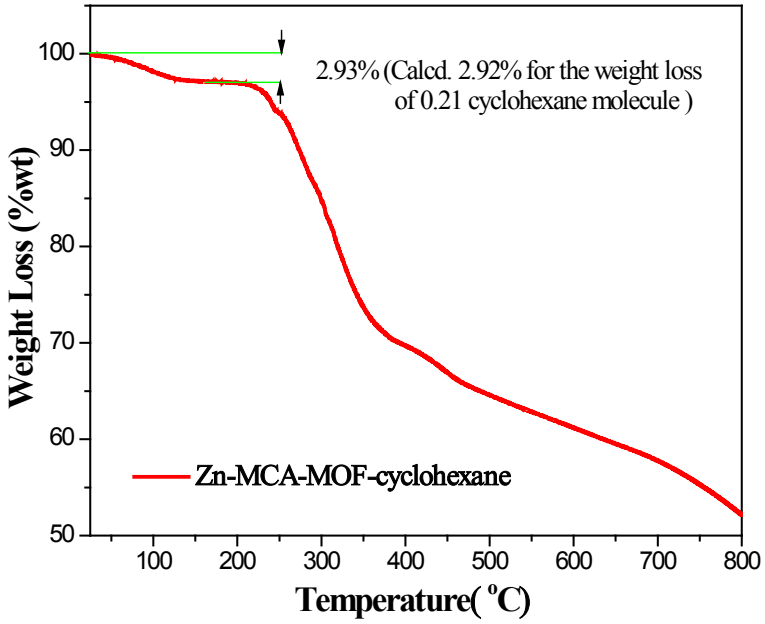

Figure S59. TG analysis of cyclohexane adsorbed form, 2⊃cyclohexane. The observed weight loss (2.93%) is the weight of 0.21 cyclohexane molecules.

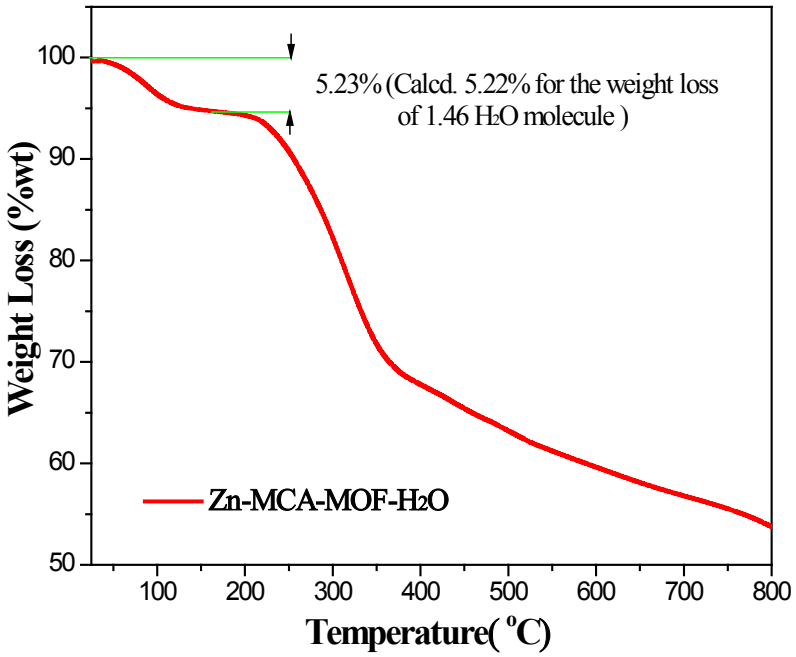

Figure S60. TG analysis of H_2O adsorbed form, 2⊃H_2O. The observed weight loss (5.23%) is the weight of 1.46 H_2O molecules.

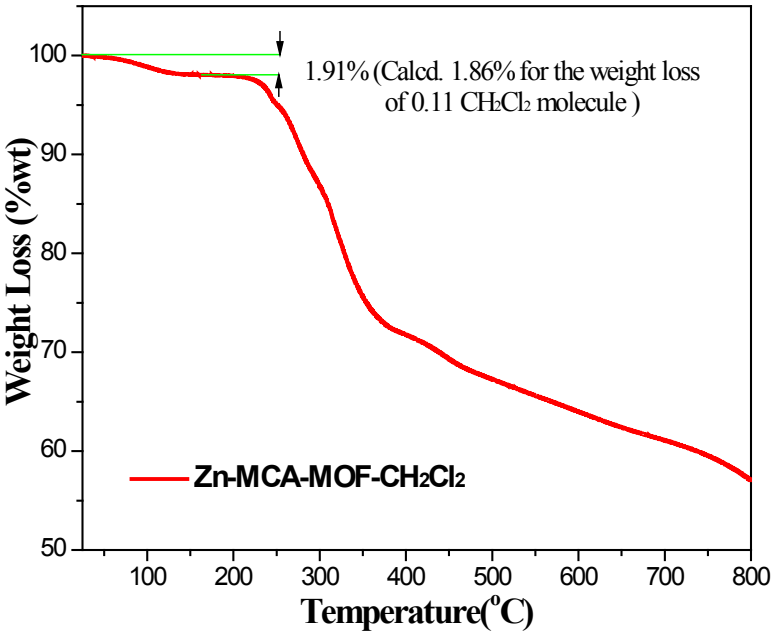

Figure S61. TG analysis of CH_2Cl_2 adsorbed form, 2⊃CH_2Cl_2. The observed weight loss (1.91%) is the weight of 0.11 CH_2Cl_2 molecules.

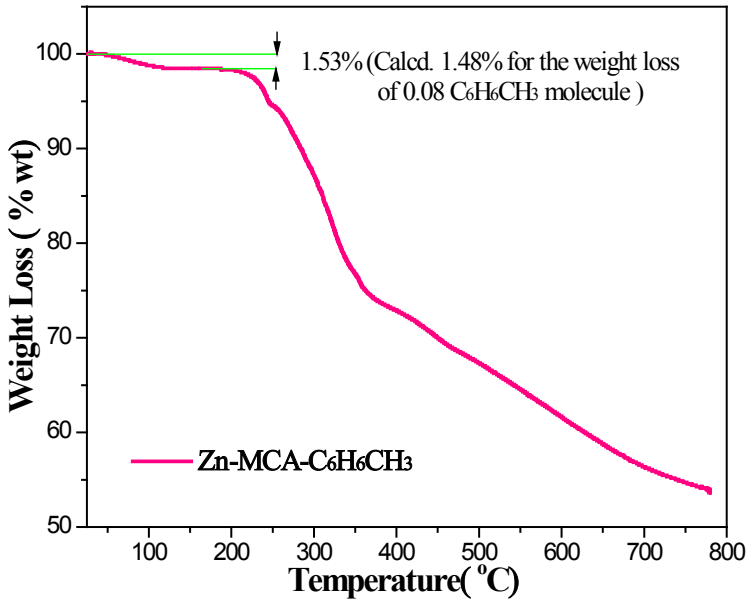

Figure S62. TG analysis of $C_6H_6CH_3$ adsorbed form, $2\supset C_6H_6CH_3$. The observed weight loss (1.53%) is the weight of 0.08 $C_6H_6CH_3$ molecules.

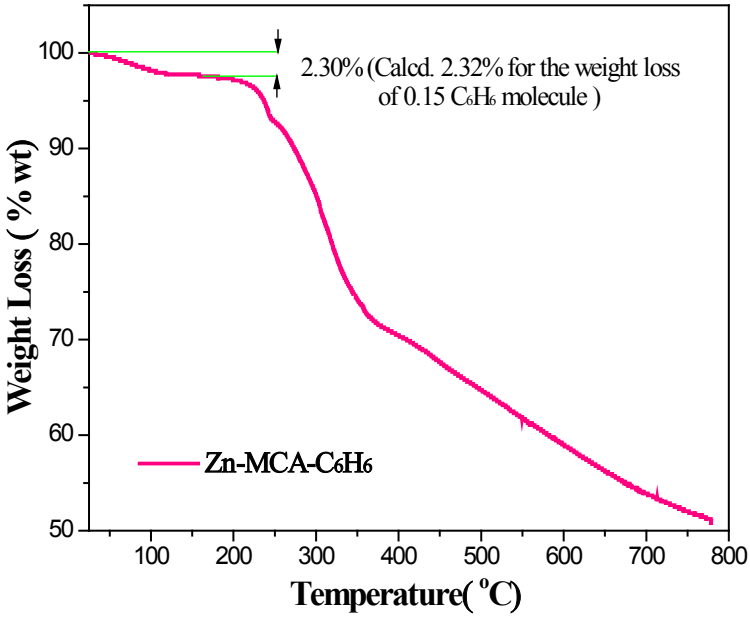

Figure S63. TG analysis of C_6H_6 adsorbed form, $2\supset C_6H_6$. The observed weight loss (2.30%) is the weight of 0.15 C_6H_6 molecules.

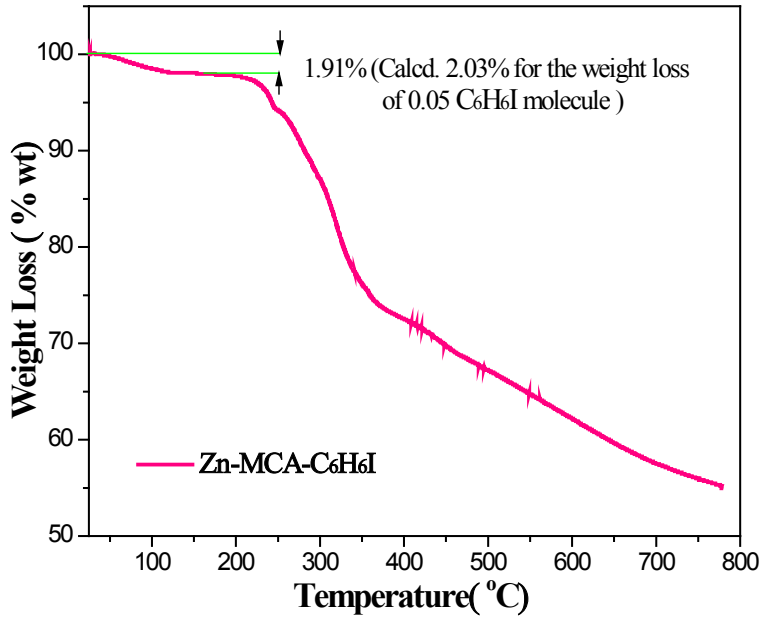

Figure S64. TG analysis of C_6H_6I adsorbed form, $2\supset C_6H_6I$. The observed weight loss (1.91%) is the weight of 0.05 C_6H_6I molecules.

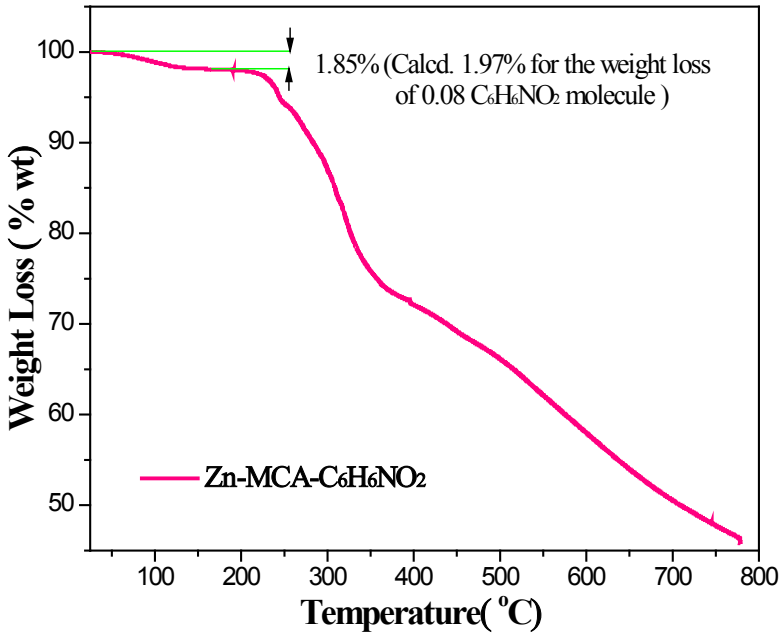

Figure S65. TG analysis of $C_6H_6NO_2$ adsorbed form, $2\supset C_6H_6NO_2$. The observed weight loss (1.85%) is the weight of 0.08 $C_6H_6NO_2$ molecules.

Section 11. Gas sorption isotherms of MOF 1a and 2a for N_2

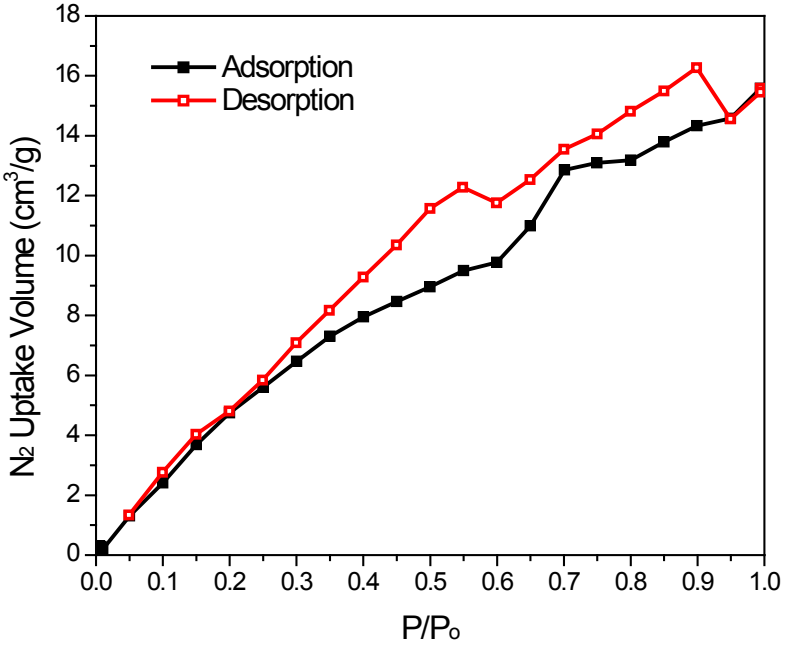

Figure S66. Gas sorption isotherms of MOF **1a** for N_2 (Surface Area = 26.982 m^2/g).

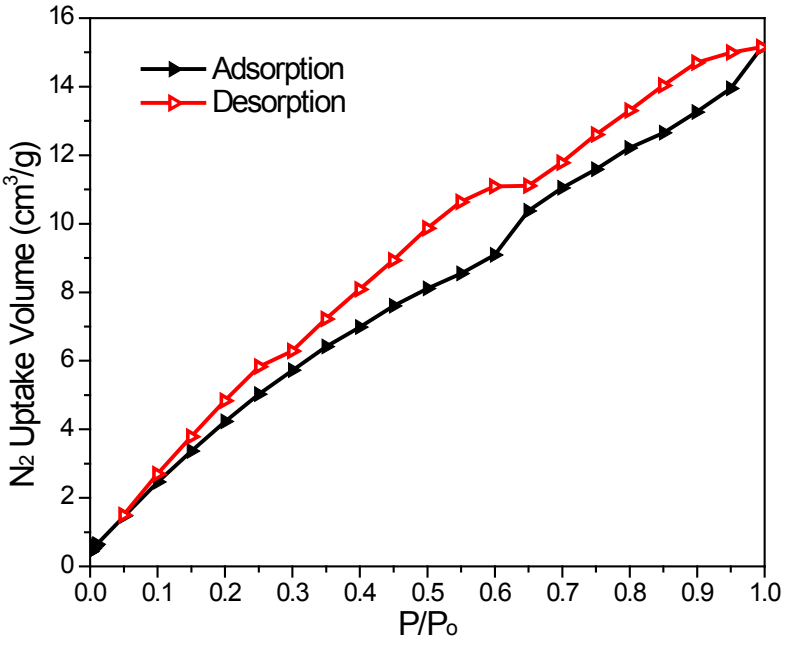

Figure S67. Gas sorption isotherms of MOF **2a** for N_2 (Surface Area = 23.542 m^2/g).